LBL-16925
EEB-L 83-07
L-77

LBL--16925

DE84 005868

TEST, EVALUATION, AND REPORT ON MERCURY ENRICHMENT FOR FLUORESCENT LAMPS

Jakob Maya, Principal Investigator*
M. Grossman, D. Rider, and R. Lagushenko, Contributors*

Lighting Systems Research
Lawrence Berkeley Laboratory
University of California
Berkeley CA 94720

October 1983

This work was supported by the Assistant Secretary for Conservation and Renewable Energy, Office of Building Energy Research and Development, Building Equipment Division of the U.S. Department of Energy under Contract No. DE-AC03-76SF0098.

*GTE Lighting Products
100 Endicott Street
Danvers MA 01923

Subcontract No. 4516910

This manuscript was printed from originals provided by the authors.

EBB

TABLE OF CONTENTS

List of Figures

TABLE OF CONTENTS (Concluded)

List of Figures

List of Tables

I. ANNUAL REPORT HIGHLIGHTS

1. A technique for dispensing minimum amounts of Hg into discharge vessels has been developed.

2. An accurate efficiency, light output and electrical parameter measurement procedure has been developed.

3. A proper data analysis procedure has been developed and adopted.

4. Efficiency improvements of 2-5% as a result of added ^{196}Hg concentrations of 1-3% have been demonstrated. These efficiency improvements have been realized in statistically meaningful sample sizes for T/12, T/9 and T/8 fluorescent lamps.

5. Cold spot temperature measurements indicate a shift of about 2°C for the optimum operation of the 3% ^{196}Hg enriched lamp (42°C compared to 40°C). This optimum, however, is not very sharp due to the flat nature of light output versus cold spot temperature curve.

6. A lower rare gas pressure appears to yield comparable efficiency improvements at lower ^{196}Hg concentrations. Definite word on this, however, needs further experimentation.

7. High frequency operation of isotopically enriched lamps indicated that the efficiency improvement due to isotopes is independent of frequency of operation.

8. A resonance radiation transport formalism developed earlier has been utilized to interpret the results.

9. A brief preliminary experiment on the relative efficiency of a fluorescent lamp due to a permanent transverse magnetic field gave 9.1% improvement.

10. Preliminary calculations on the relative merits of photoionization versus photochemical methods of ^{196}Hg isotope separation schemes indicate the superiority of the latter from the throughput and efficiency points of view.

11. A photochemical isotope separation flow reactor and excitation source has been designed and built.

12. Enrichment factors for ^{196}Hg up to 32 in a single pass have been achieved, (i.e., natural concentration of 0.146% increased to 4.7%).

13. Product recovery procedures have been dealt with and some progress made.

II. INTRODUCTION

This report summarizes effects of utilizing mercury enriched in ^{196}Hg on fluorescent lamp efficacy and operational characteristics and results of enrichment of ^{196}Hg via a photochemical reaction technique. The central theme of the lamp studies is the measurement of lumen efficacy and electrical operating points as a function of isotopic distribution within individual lamps. That is, test lamps are first run in natural mercury, then mercury containing ^{196}Hg is dispensed within the lamp. A comparison of the lamp operation before and after ^{196}Hg dispensing is made to find the effects of altered isotopic distribution on lamp operation. The lamp studies can be divided into the categories shown in Table 1.

Two additional topics were briefly looked into, as indicated in Table 1; effects of d.c. magnetic fields applied transverse to the lamp current flow and effects of high frequency lamp operation.

TABLE 1. OUTLINE OF LAMP STUDIES

1. Hg Dispensing
    - 1.1 Ampul Forming and Filling
    - 1.2 Ampul and Lamp Processing
    - 1.3 Ampul Opening
    - 1.4 Comparison of Predicted and Measured ^{196}Hg Concentration
2. Lamp Measurements
    - 2.1 Luminous Efficacy
    - 2.2 Water Bath
    - 2.3 Lamp Types Studied
3. Data Analysis
    - 3.1 "100 Hour" Method
    - 3.2 Least Square Fit (lsf) Method
4. Summary and Discussion of Results
5. Magnetic Field Studies
6. High Frequency Studies

Photochemical enrichment was oriented toward establishing feasibility of using a static reactor or flow reactor to obtain enrichments of ^{196}Hg of about a factor of thirty starting with natural mercury as the feed stock. Most of the work where substantial enrichment was observed was carried out on a fairly simple flow reactor. Promising results have been obtained from the point of view of very high enrichments, though additional measurements of yield and utilization factor need to be carried out and overall enrichment processes optimized.

The photochemical work will be described as outlined in Table 2.

TABLE 2. SUMMARY OUTLINE OF PHOTOCHEMICAL ENRICHMENT

1. Photoionization versus Photochemical Method Calculation
2. Utilization of Previous Work
    - 2.1 Gunning, et al
    - 2.2 Webster and Zare
    - 2.3 Present Direction
3. Excitation Lamp
    - 3.1 Fabry Perot Interferometer
    - 3.2 Microwave Lamp Construction
    - 3.3 Lamp Spectra
    - 3.4 Mercury Filter
    - 3.5 Optimizing Lamp Filter Combination
4. Static Reactor Experiments
    - 4.1 Equipment
    - 4.2 Reactions Studied and Procedures
    - 4.3 Summary
5. Flow Reactor Experiments
    - 5.1 Equipment
    - 5.2 Procedures
6. Collection Methods
7. Sample Analysis
8. Summary of Flow Reactor Results

III. LAMP STUDIES

1. Hg Dispensing

Due to the high cost of ^{196}Hg, minimum quantities of ^{196}Hg have been used in these lamp studies. Figure 1 shows the method by which thin tubes of infrared absorbing glass are prepared for forming into capsules in order to dispense approximately 0.2 mg of Hg enriched in ^{196}Hg. One end of the tube is sealed while the other end is left open for filling with Hg via a syringe. Electrical heater wire is wound, as shown, prior to Hg filling. Before connecting the heater wire to a power supply, the tube is evacuated, Ar backfilled, and flame sealed to form an enclosed tube containing Ar, liquid Hg and Hg vapor. Figure 2 shows the result of applying power to the heater wire while the tube-wire assembly is within an oven. Care is taken to ensure complete vaporization of the Hg yet maintaining the total pressure below that outside of the tube.

The capsules formed are then mounted on filament support wires in phosphor coated lamps and then the lamps processed.

Capsules containing 2 to 4 mg of natural Hg are formed by evacuating a tube sealed at one end and preloaded with Hg. The evacuated tube is Ar backfilled and flame sealed into a small ampule. This ampule is then also mounted on filament support wires prior to lamp processing.

Thus, two types of capsules are used in these experiments. One type contains approximately either 2 mg or 4 mg of natural Hg while the other type contains approximately 0.2 mg of natural Hg or 0.2 Hg enriched to about 35% ^{196}Hg. The test lamps are always processed free of Hg and then aged after opening one of 2 or 4 mg capsules of natural Hg. The test lamps always contain one or more 0.2 mg Hg capsules with Hg enriched in ^{196}Hg. One group of control lamps are identical to test lamps but contain natural Hg in the 0.2 mg capsules instead of ^{196}Hg enriched mercury. A second set of control lamps have only 2 mg or 4 mg of natural Hg contained in a capsule while a third group of control lamps have natural Hg dispensed into them during initial processing.

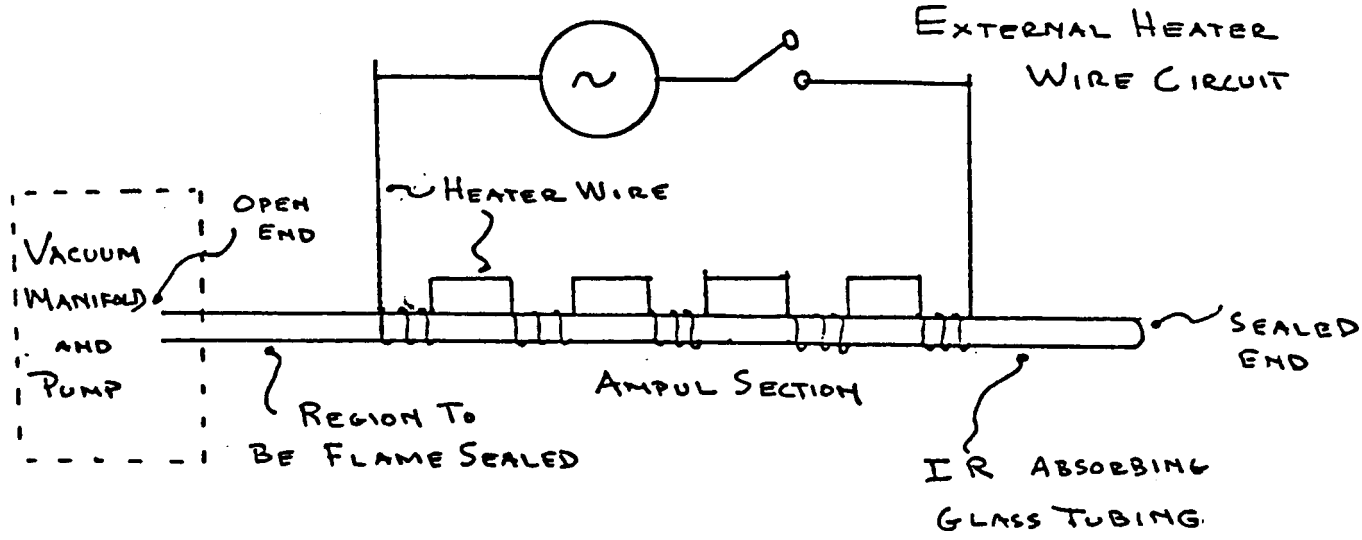

Figure 1. Preparation of Tube for Sectioning into Ampuls.

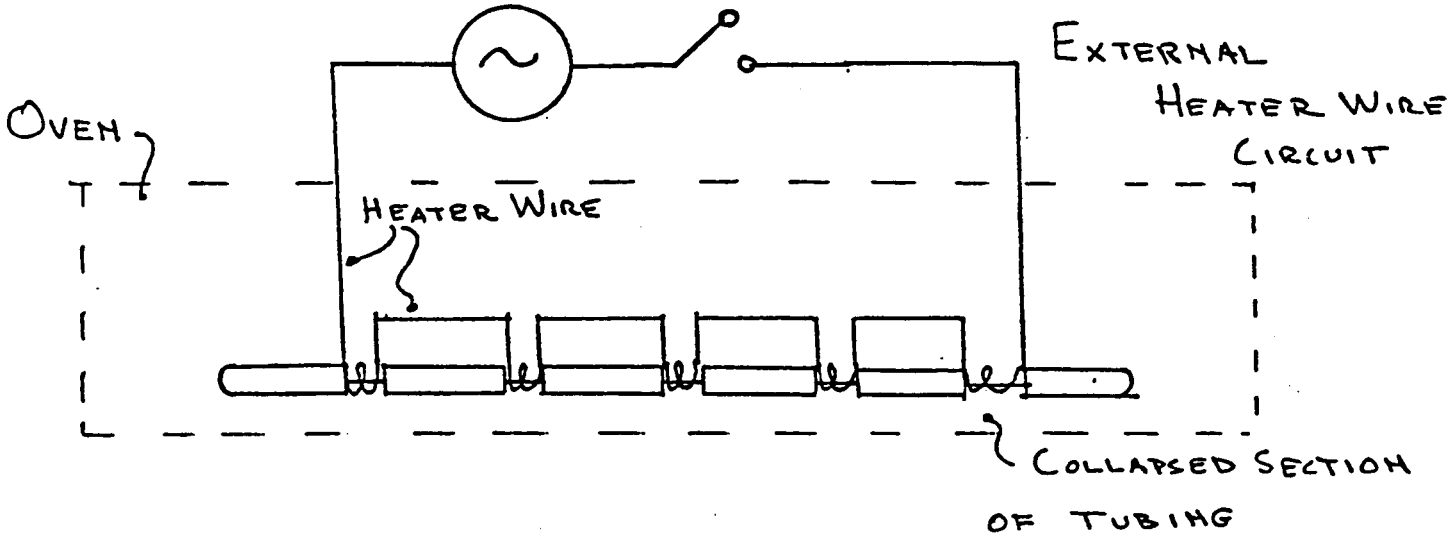

Figure 2. Ampul Sections After Power Applied to Heater Wire.

Pulsed infrared or ruby lasers proved fairly effective in opening both types of capsules.

A second method that was developed utilizes incandescent projection lamps. In the case of the 2 mg or 4 mg capsule, a single projection lamp was adequate to open the capsule whereas in the case of the 0.2 mg capsule, two lamps are required.

After the lamp measurements are completed, the test lamps are opened in such a way so as to introduce the contained Hg into a mass spectrometer for isotopic analysis. Table 3 shows the results. As indicated, most of the measured ^{196}Hg quantities tended to be somewhat higher than predicted which may be due to Hg depletion mechanism within the lamp during the first 100 hours of lamp operation prior to introducing the Hg enriched in ^{196}Hg.

2. Lamp Measurements

Two basic types of lamp measurements were carried out, luminous efficacy and water bath measurements. Luminous efficacy measurements utilized a 2.4m integrating sphere, the results of which were used to evaluate the changes in lamp lumen output, efficacy, and operating point for different ^{196}Hg concentrations. Water bath measurements in which the entire lamp is submerged in a volume of circulating water were carried out in order to determine the variation in lamp efficacy as a function of cold spot temperature for different isotopic distributions. An EG&G photometer with photopic filter was used to measure lamp output from one section of the lamp.

Table 4 indicates the lamp types studied and some of their characteristics.

3. Data Analysis

The integrating sphere measurements were carried out over a period of approximately 100 to 200 hour increments. All integrating sphere measurements were carried out in accordance with accepted IES procedures and calibrations traceable to NBS standards. Initial measurements were carried out for lamps operating only with natural mercury. Two separate test

TABLE 3. MEASURED AND PREDICTED ^{196}Hg CONCENTRATIONS.

Lamp ID	Percent Enrichment ^{196}Hg	
	Measured	Predicted
F40T12-1	4.9	4.1
-3	3.2	4.1
-7	3.8	2.7
-8	3.7	2.7
-10-7	3.3	2.9
-10-8	3.0	2.9
-11-1*	10.2	5.3
-11-3*	5.6	2.9
F34T12-12-3	3.0	2.9
-12-4	3.2	2.9
-12-5	4.2	4.1
F32T9-27-7	3.1	4.1
27-8	4.0	2.9
27-9	5.4	4.1
27-10	1.7	1.5
F32T8-25-7	4.6	2.9

*2 mg initially dispensed natural Hg. All others 4 mg.

TABLE 4. CHARACTERISTICS OF LAMP TYPES STUDIED.

Lamp Type	Sample Size	V_l(V)	I_l(A)	Gas Fill
F40T/12	24	103	430	2.3t Ar
F34T/12	37	80	460	1.3t Kr + 0.2t Ar
F32T/9	8	80	430	2.5t Ar
F32T/8	15	135	260	2.5t Ar

procedures were carried out on different lamp groups. The "100 hour" comparison method utilized the efficacy measurements of control and test lamps at 100 hours, all lamps running in natural mercury. After the 100 hour efficacy measurements, capsules containing 0.2 mg of mercury enriched in ^{196}Hg were opened in the test lamps. Efficacy measurements then continued to be carried out for the test and control lamps. Because of the normal maintenance of fluorescent lamps it was necessary to distinguish between maintenance decay and changes due to isotopic alteration. This change was taken into account by observing the maintenance of the control lamps relative to 100 hours. The precise definition of improvement due to isotopic alteration is shown in Table 5. As noted, the measured improvement fluctuates during time, at least in part due to the normal variations in lumen efficacy measurements. As indicated in Table 5, the time at which the maximum improvement is observed is chosen for each lamp.

TABLE 5. DEFINITION OF PERCENT IMPROVEMENT OF LUMEN OUTPUT FOR "100" HOUR ANALYSIS.

$$P_{LUM} = \frac{\Delta\ LUM_E - \overline{\Delta\ LUM}_C}{\overline{LUM}_C}$$

where Δ LUM = Lumen output at t_m minus lumen output at t = 100 hours for each test lamp.

$\overline{LUM}_C$ = Average lumen output of control lamps at time t_m.

$\overline{\Delta LUM}_C$ = Lumen output at t_m minus lumen output at t = 100 hours averaged over all control lamps.

The time t_m is chosen to give a maximum value of P_{LUM} for each test lamp. Furthermore, P_{LUM} is an average value corresponding to lamps having the same concentration of ^{196}Hg.

A least square fit (lsf) analyses has been developed to effectively average normal lamp and measurement fluctuations which might distort changes in lamp operation due to isotopic alteration. Essentially, the lamp maintenance curve is fitted via lsf to the function

$$I = I_0 \exp-(t/\tau)^{\frac{1}{2}}$$

using luminous efficacy data for test lamps running initially with natural Hg. A second fit is carried out after the isotopic alteration. The shift in these two maintenance curves represents the lumen improvement due to isotopic alteration and is shown schematically in Figure 3.

The lsf analyses is being applied to F34T12 lamps and F32T9 lamps still under test. Some preliminary results of these measurements will be given. Figure 4 shows that a reasonably good maintenance fit can be made with F40T12 lamps running in natural Hg using the function indicated above. It is noted that zero hour efficacy data is not used in the lsf method, thereby, resulting in a two parameter lsf analysis.

The water bath measurements determined the variation of LPW as a function of lamp cold spot temperature. For each lamp LPW refers to the measured lumen output from one section of the lamp divided by total arc power (a rapid start reference ballast was used). These values, when compared to the value at 40°C, are referred to as relative LPW.

In carrying out the lumen data analyses via the least square fit method, voltage shifts could be determined for the F34T12 lamps after capsules containing Hg enriched in ^{196}Hg were opened. For the first 200 or 300 hours of lamp operation in natural Hg, the lamp voltage readings were consistently falling and so these were not included in the measured voltage shift. After about 300 hours the voltage readings appeared to be stable. Thus, from 300 hours to about 650 hours, arc voltage, arc current, and arc power readings were considered representative of stabilized lamps in natural Hg. Mean values were obtained for test and control lamp and their values compared to corresponding mean values after capsules containing Hg enriched in ^{196}Hg were opened.

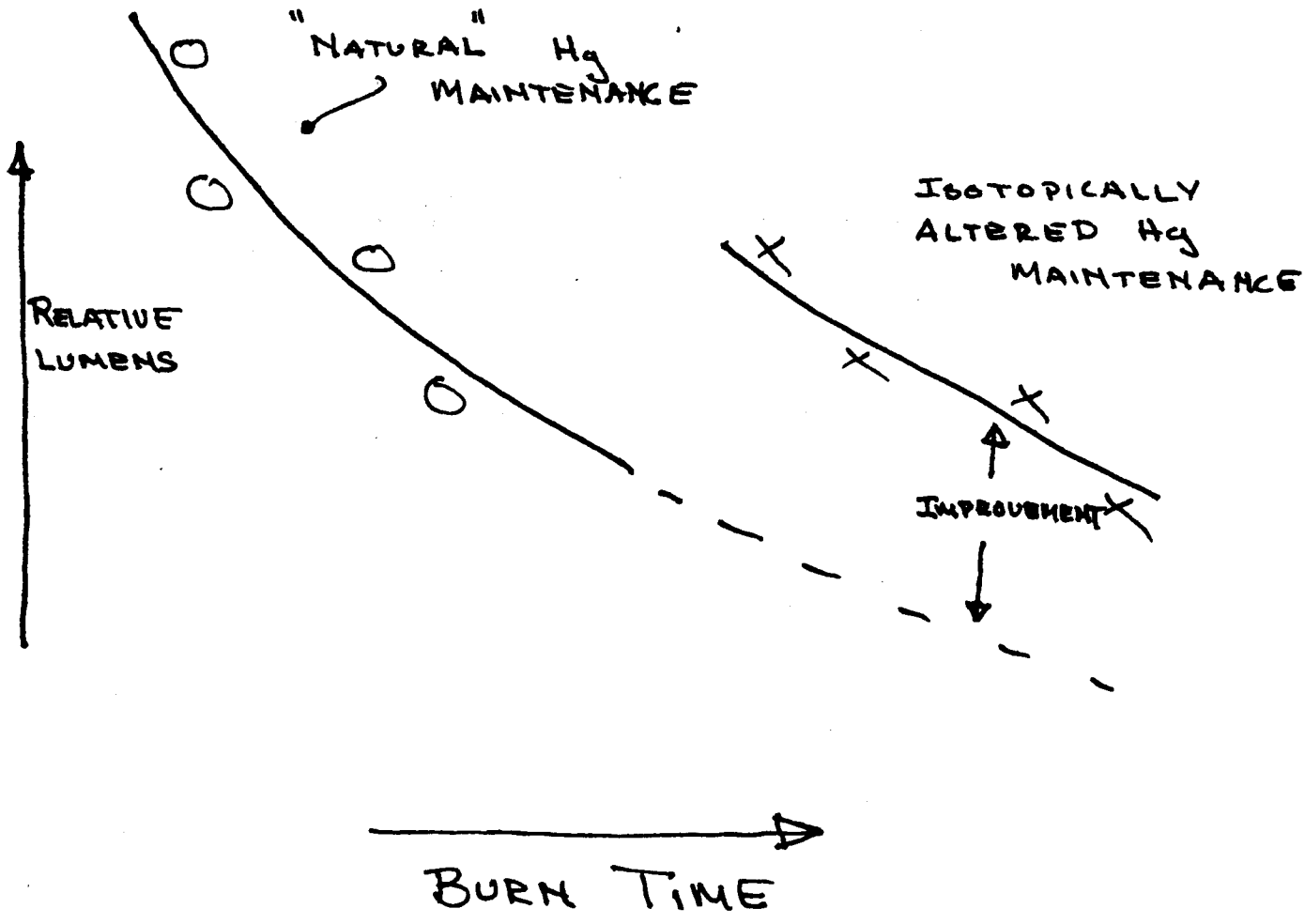

Figure 3. Principle of Least Square Fit Analysis.

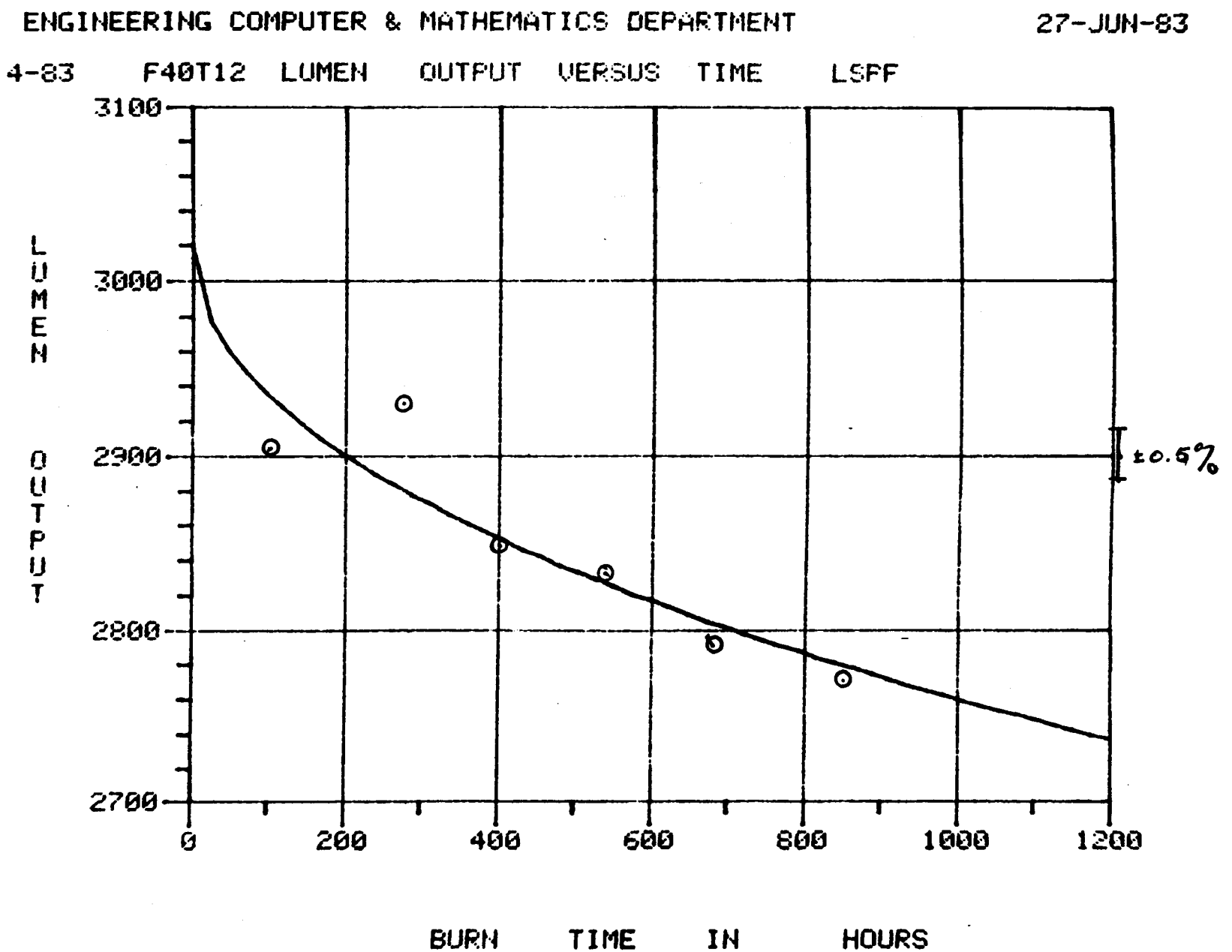

Figure 4. Least Square Fit of Natural Mercury F40T12 Lamps.

4. Summary and Discussion of Results

Table 6 summarizes the results of the "100 hour" analysis method. As noted, typical T12 improvements are 2 to 5% while T8 and T9 improvements are of the order of 1 to 4%.

Figures 5 and 6 show some of the results of the least square fit analysis for a F34T12 control lamp and a F34T12 test lamp. The points on the graph shown as circles represent lamp operation in natural mercury. The points shown as plus signs represent the lamp operation after capsules containing 0.2 mg of Hg were opened in the lamp. In the case of Control Lamp 3, these capsules contained natural Hg, whereas, for the test lamps, they contained mercury enriched in ^{196}Hg. The ^{196}Hg concentration in Test Lamp 6 is 3%. The solid line is a least square fit of the maintenance data prior to opening the 0.2 mg capsules.

As noted in Figures 5 and 6, the control lamp maintenance as well as the test lamp maintenance shows an increase in lumen output after the 0.2 mg capsules are opened. Examination of similar curves for control lamps with no capsules, however, show increases similar to Control Lamp 3. As a preliminary estimate, it appears that about 20% of the improvement in the F34T12 test lamps is due to a systemic measurement error. At the present time, we do not know where this increase is coming from. We can only speculate that it may be due to some non-equilibrium effects. Whatever the origin, however, the improvement due to ^{196}Hg takes this 20% increase into account.

Preliminary results of the lsf method are in excellent agreement with the results of the "100 hour" method. Therefore, we feel confident that our results are real and not the result of some data analysis coincidence. Overall, however, we feel that the lsf method is a more conservative and technically proper way of analyzing the data.

Figures 7 and 8 are corresponding data and lsf analyses for F32T9 lamps. Here the set of control and test lamps have only one 0.2 mg capsule opened and in continuing tests, additional capsules will be opened to observe the effects of further ^{196}Hg enrichment.

TABLE 6. PERCENT IMPROVEMENT IN LUMEN OUTPUT AND LPW AS A FUNCTION OF ISOTOPIC DISTRIBUTION USING "100 HOUR" ANALYSIS OF MAINTENANCE DATA.

Lamp Type \ ^{196}Hg Concentration in %	0.6-1.5	1.6-2.5	2.6-3.5	3.6-4.5	4.6-5.5	5.6-6.5	9.6-10.5
Lumen Improvement							
F32T8	1.8				1.2		
F32T9		2.6	2.6	3.6	0.5		
F34T12		3.1	1.9				
F40T12		2.9	5.4	2.3	3.3		2.3
LPW Improvement							
F32T8	1.5				0.5		
F32T9		0.4	3.9	3.2	-0.9		
F34T12		4.6	2.3				
F40T12		2.3	3.8	4.6	3.2		0.3

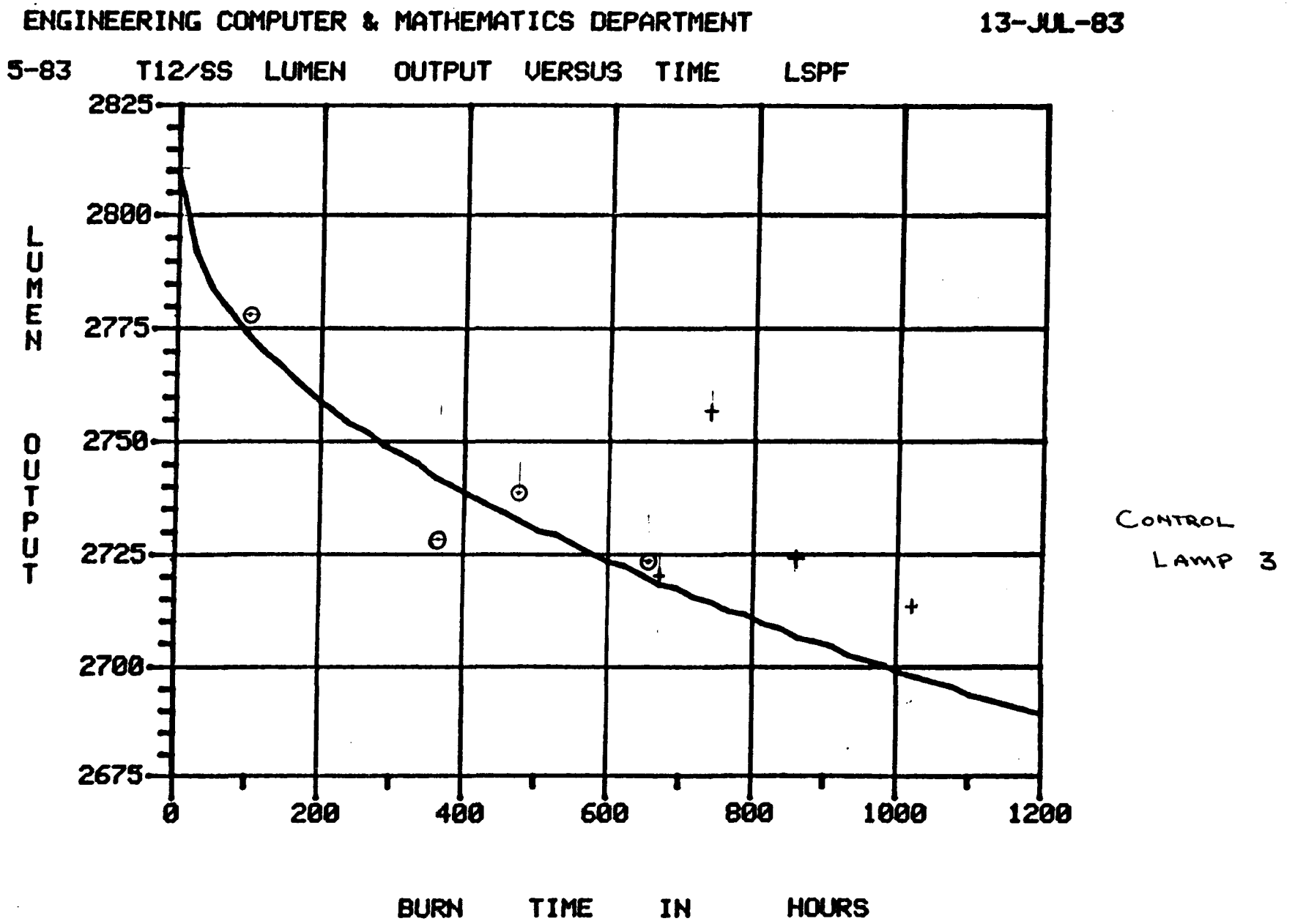

Figure 5. Typical Control Lamp Maintenance for F34T12.

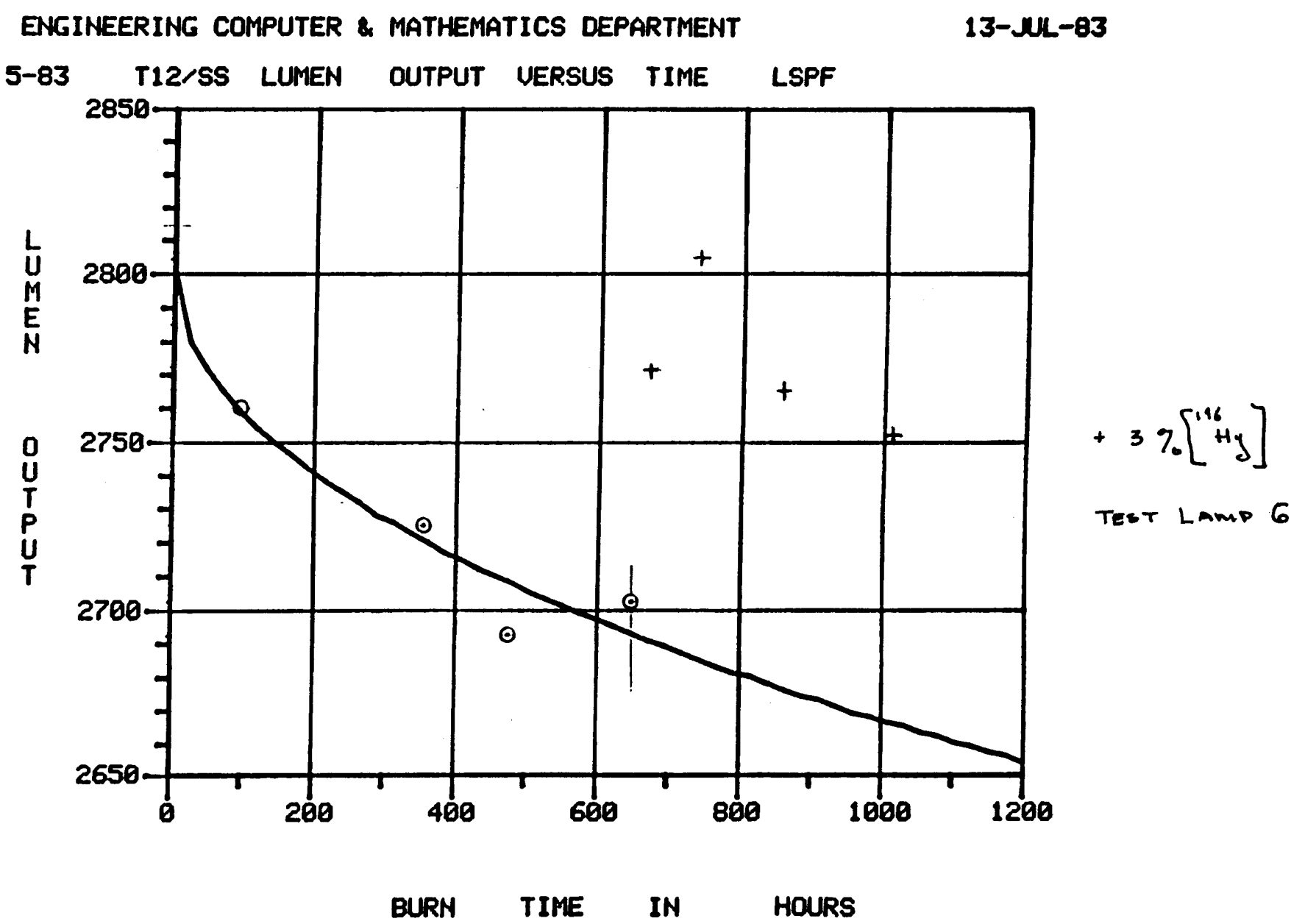

Figure 6. Typical Test Lamp Maintenance F34T12.

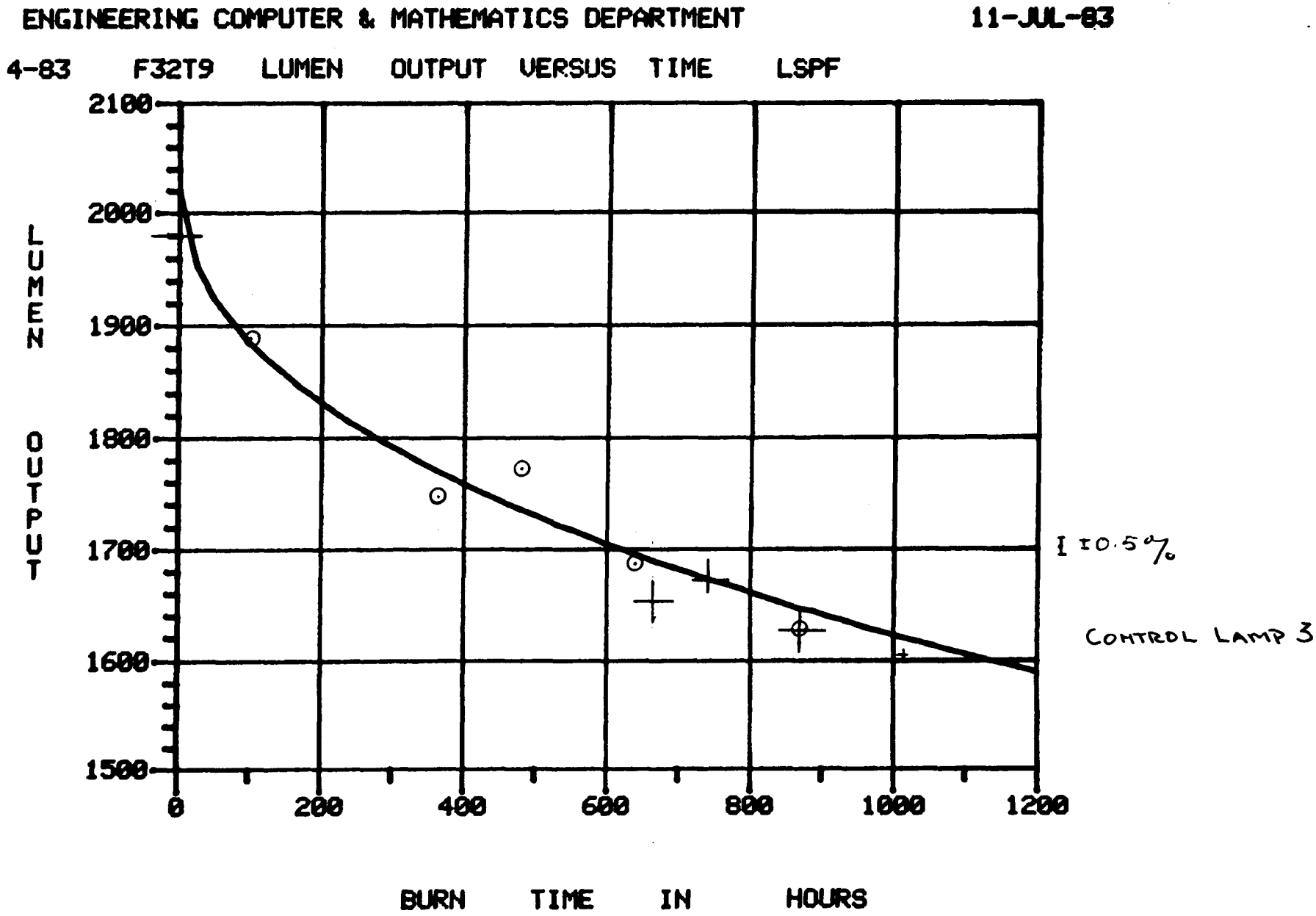

Figure 7. Typical Control Lamp Maintenance F32T9.

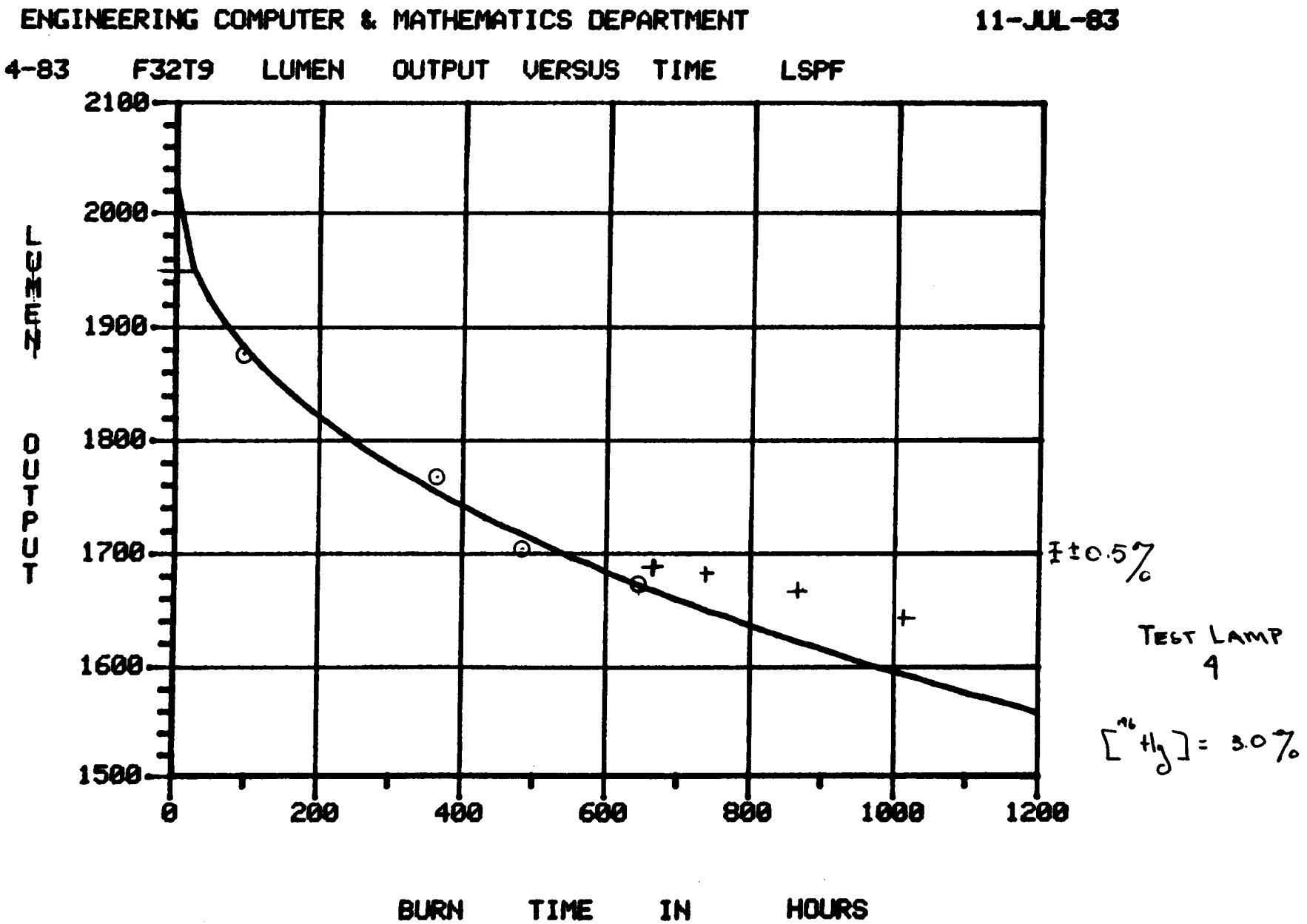

Figure 8. Typical Test Lamp Maintenance F32T9.

Preliminary analyses indicates a 0.5 to 1.0 volt increase in the F34T12 test lamp arc voltage at constant current, approximately 430 ma. We estimate the accuracy of our results to be about ∓ 1% both for the LPW and lumen improvement data. Looking at the data it would appear the maximum LPW and lumen improvement for F34T12 takes place at a lower ^{196}Hg than the F40T12. This may be due to the fact that F34T12 contains only 1.5 torr rare gas (87% Kr, 13% Ar) compared to 3.0 torr in the F40T12 (100% Ar). Since pressure broadening would be less at 1.5 torr (∿ a factor of 2 less) rare gas the effect of ^{196}Hg addition may manifest itself at a lower concentration. This would seem plausible in view of the fact that pressure broadening of the hyperfine components is the dominant broadening mechanism.

Results of the water bath experiments for F32T8 and F40T12 lamps are shown in Figures 9 and 10. One notes that at low enough temperatures ≅ 20°C, the LPW curves of the control and test lamps show no difference. At minimum LPW, the F40T12 lamps showed no shift in the temperature at which the peak LPW occurs but the F32T8 apparently do. A comparison of these results to theoretical models is being carried out as well as measurements for F32T9 and F34T12 lamps.

5. Magnetic Field Studies

Figure 11 shows the configuration used to test the effect of a transverse dc magnetic field on lumen efficacy of a F14T12 lamp. The magnetic field transverse (longitudinal component < 10 gauss) had a large gradient. The field varied from about 600 gauss to 40 gauss across the median plane of the lamp discharge. Measurements of the 2537Å hyperfine structure clearly showed a "filling in" of regions of the spectra. This may be due to Zeeman splitting or other discharge effects to be investigated later. This filling can account for at least part of the improvement in the LPW as shown in Table 7.

6. High Frequency Operation

F32T8 (Octron) and F34T12 (SuperSaver) test and control lamps were operated via a high frequency power supply. As shown in Table 8, the effect of isotopic enrichment was "carried over" from 60 Hz operation to high frequency

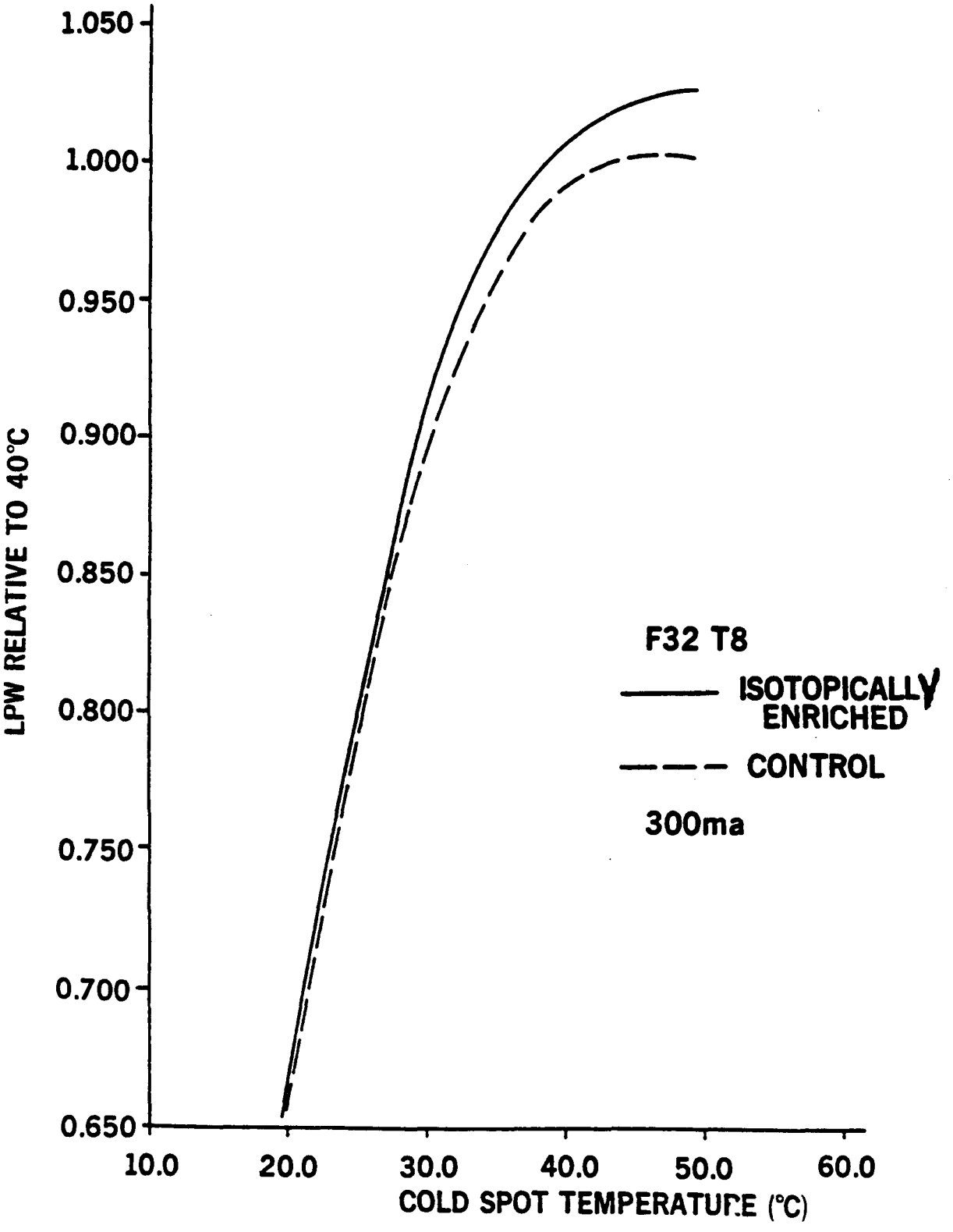

Figure 9. LPW as a function of cold spot temperature relative to 40°C.

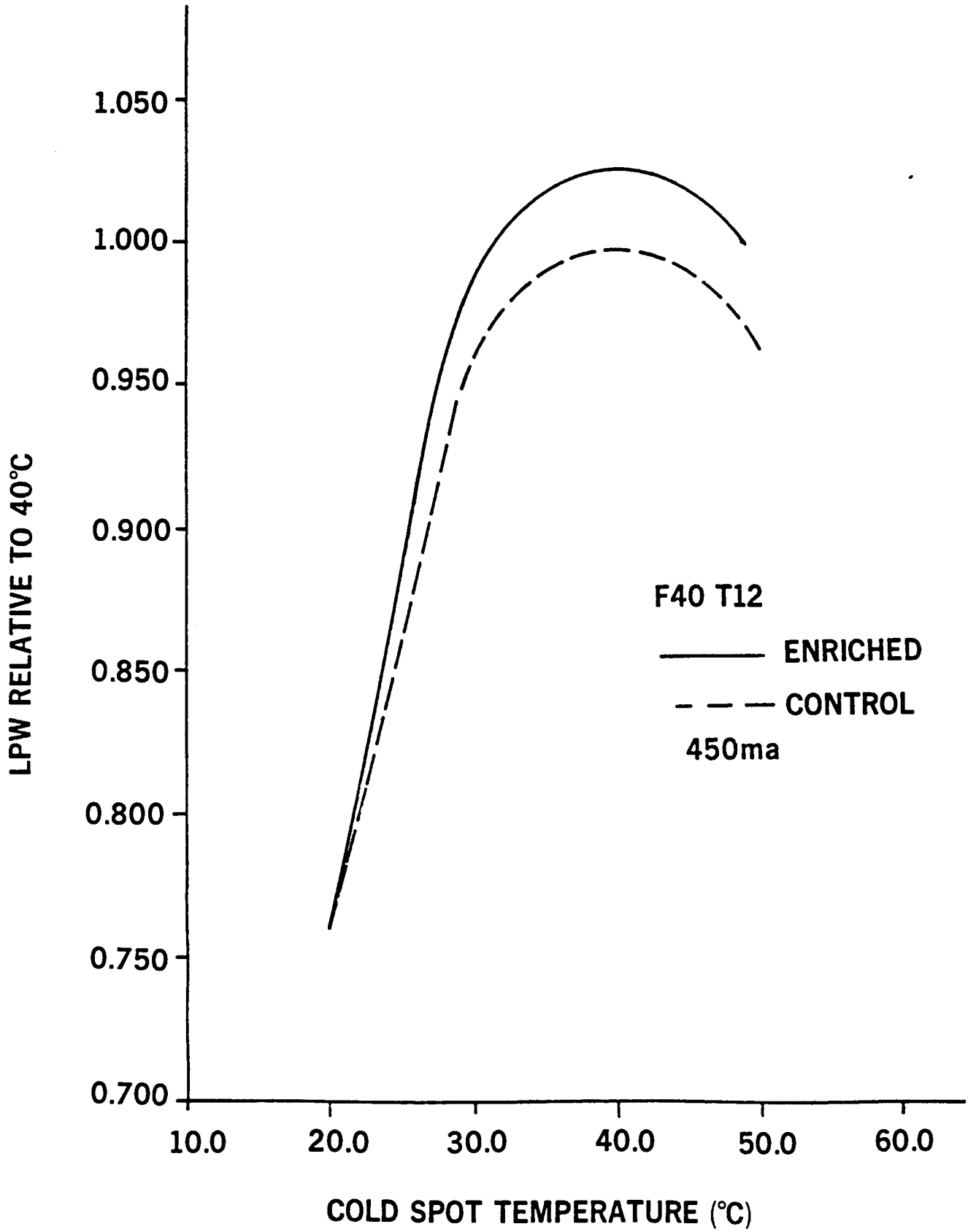

Figure 10. LPW as a function of cold spot temperature relative to 40°C.

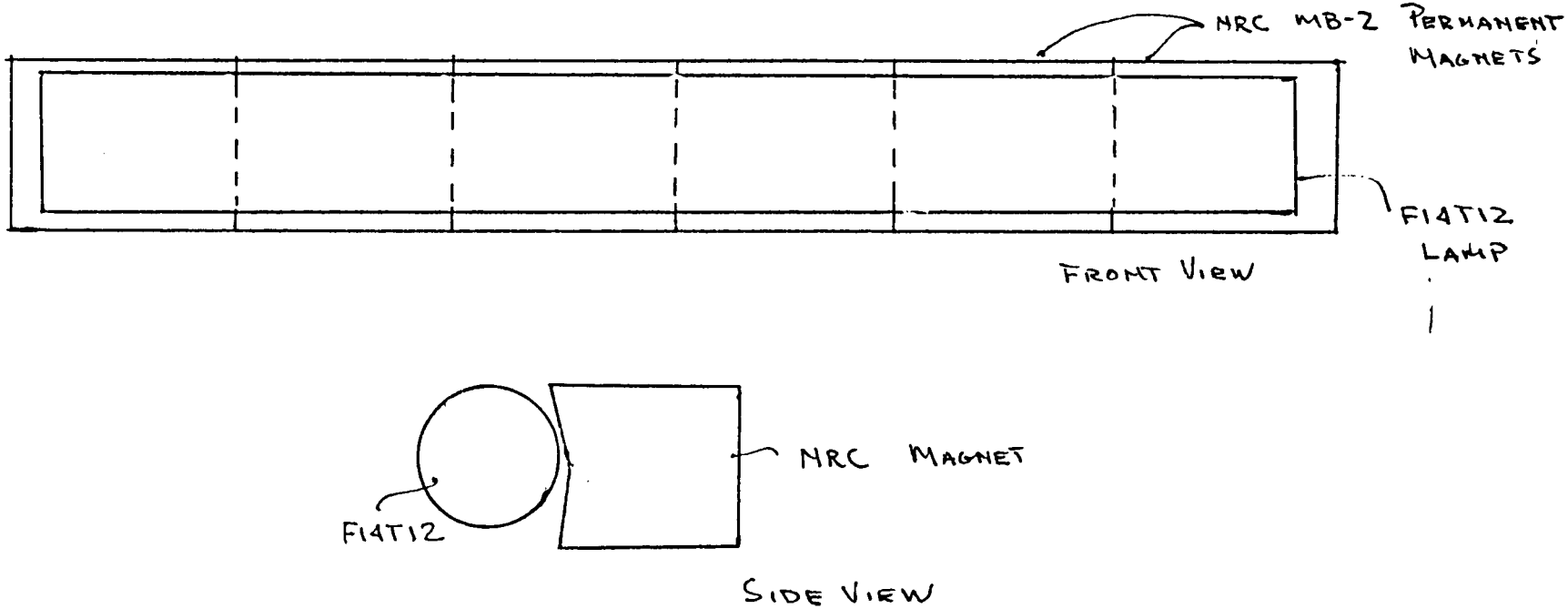

Figure 11. Magnet and Lamp Configuration as tested in 2.4 meter Integrated Sphere.

TABLE 7. PERMANENT TRANSVERSE MAGNETIC FIELD

Magnet State	V_{REF}	I_L	V_L	W_L	Relative Lumen Output	LPW	LPW Change Relative To Magnet Off At Start
	Volts	mA	Volts	Watts	ARB Units	ARB	%
Off-start	118	379	40.08	14.51	591	40.8	0
On	118	377	41.61	14.88	663	44.5	9.1

TABLE 8. IMPROVEMENT IN LPW FOR HIGH FREQUENCY OPERATION OF CONTROL AND ^{196}Hg ENRICHED LAMPS.

LAMP TYPE		NORMALIZED LPW 60 Hz	NORMALIZED LPW 30 K Hz	% IMPROVEMENT DUE TO HF
OCTRON	CONTROL	100	104.2	4.2
	~1% ^{196}Hg ENRICHED	102	107.1	4.9
F40 T/12 SUPERSAVER	CONTROL	100	110.7	10.7
	2.6 % ^{196}Hg ENRICHED	103.1	114.5	11.1

operation at 30 KHz. Clearly, the isotopic effect and high frequency effects one additive. This is encouraging in view of the potential of using high frequency electronic ballasts in the future.

IV. ISOTOPE SEPARATION

1. Photoionization versus Photochemical Method Calculations

A method of isotope separation by selective two step (STS) photoionization process is now widely discussed in the literature (1,2 and 3).

In the following, we report our preliminary estimates on applications of this method to the mercury isotope separation. As one knows, STS photoionization process is carried out by two photons of energies $h\nu_e < E_i$ (E_i is the ionization energy of the mercury atom in the ground state) the overall selectivity of ionization can be maintained. The selectivity is affected by the excitation and charge transfer reactions:

$$Hg_s^* (6^3P_1) + Hg(^1S_o) \rightarrow Hg_s(6^1S_o) + Hg^*(6^3P_1)$$

$$Hg_s^+ + Hg(6^1S_o) \rightarrow Hg_s(6^1S_o) + Hg^+$$

Here the index s indicates a selected mercury isotope. To accomplish the separation, ions may be extracted by an electric field. In the following we have accepted as a first approximation that the mass of the separated isotope is equal to the mass of the isotopic ion coming up to the collecting electrode. Calculations have been done for the case of the ^{196}Hg - isotope assuming that 10^5 gm of ^{196}Hg/yr is needed. In that case, one has to process about 10^8 gm of Hg/yr.

We have considered possibilities of excitation and ionization both by lamps and by laser beams. We list below basic constants used in our calculations:

$A = 10^7\ sec^{-1}$ = the radiative transition probability of 6^3P_1 - state

$\sigma_a = 5 \times 10^{-13}\ cm^2$ = the photoabsorption cross-section of 6^3P_1 - state

$K_o = 5 \times 10^{-13} \times N_s\ cm^{-1}$ = the center of line absorption coefficient of the mercury 2537 - line

N_s, cm^{-3} = the number density of selected mercury isotope

σ_{et} = $10^{-13} cm^2$ = the cross-section of the excitation transfer

σ_{ct} = $10^{-14} cm^2$ = the cross-section of the charge transfer

σ_i = $10^{-18} cm^2$ = the photoionization cross-section.

a. Excitation and Ionization by Lamps

Idealized set-up for this case is given in Figure 12. Consideration of the full amount of mercury which has to be processed per year dictates the following parameters for the set-up. L = 600 cm, H = 600 cm, D = 6 cm with the flow velocity $v_o = 10^4$ cm/sec and the mercury pressure $P_{Hg} = 10^{-2}$ torr. At such conditions $K_o D = 1$ and the trapping of the 2537 - radiation particular to the ^{196}Hg - isotope can be neglected to a first approximation.

Assuming steady-state conditions, one can evaluate the separation efficiency based on the balance equations for ion and 6^3P_1 - state population as follows:

$$\sigma_a I_e N_s / h\nu_e = (A + v_a \sigma_{ct} N + \sigma_i I_i / h\nu_i) N_s^*$$

$$\sigma_i I_i N_s^* / h\nu_i = (v_a \sigma_{ct} N + 1/T) N_i^+$$

Here T is the effective time of ion extraction to the collector which can be estimated as $T = D/v_p$ where v_p is the ion drift velocity, v_a is the atom velocity, I_e and I_i are the energy flux densities for the excitation and ionization radiation, N is the full mercury number density. The total ^{196}Hg isotope enrichment per year can be expressed as:

$$M = 1 \times 10^{-14} (N_i^+ / T) LHD \text{ gm/yr}$$

$$= 1 \times 10^{-14} LHD \frac{\sigma_a (I_e / h\nu_e) N_s \sigma_i I_i / h\nu_i)}{(A + v_a \sigma_{et} N + \sigma_i I_i / h\nu_i)(1 + v_a \sigma_{ct} NT)} \text{ gm/yr}$$

For the case of $I_e = 0.1$ w/cm^2, $I_i = 0.1$ w/cm^2, $h\nu_e = 4.9$ volt, $h\nu_i = 6$ volt, $P_{Hg} = 10^{-2}$ torr, L = 600 cm, D = 6 cm, H = 600 cm, this gives

$$M = \frac{7.6}{(1 + v_2 \sigma_{ct} NT)} \text{ gm/yr}$$

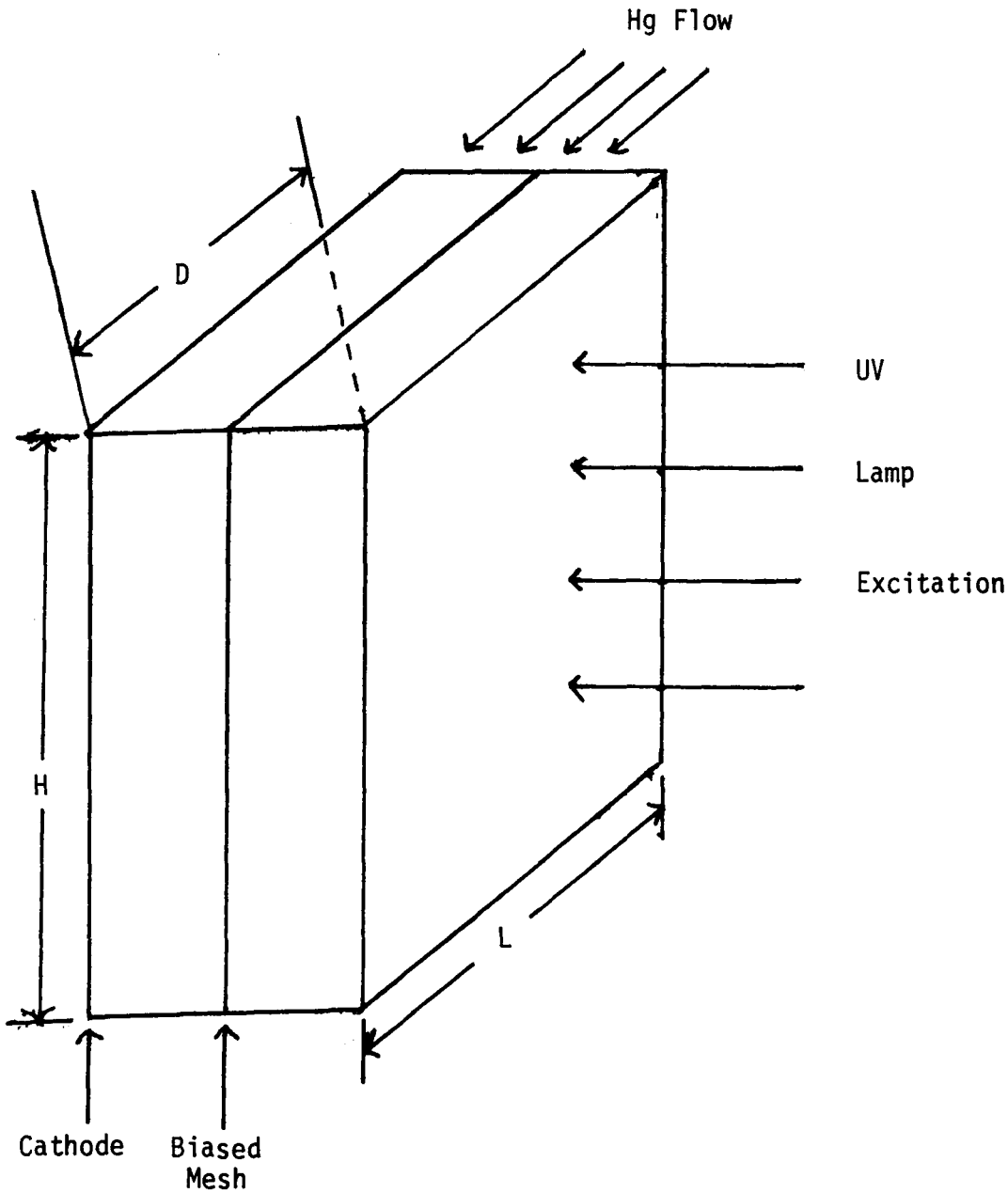

Figure 12. Idealized set-up for preliminary lamp photoionization calculations.

This result indicates that the ^{196}Hg separated by lamps using the photoionization scheme falls far below the required amounts by many orders of magnitude.

b. Excitation and Ionization by Powerful Laser Pulses

A schematic of an idealized set-up for these calculations is shown in Figure 13. The balance equations for the population of the ground state, excited state and ionic state of mercury isotopes can be written as follows:

$$dN_s/dt = - \sigma_a I_e N_s/h\nu_e + (r\sigma_a I_e/h\nu_e + A + v_a\sigma_{et}N)N_s^*$$
$$dN_s^*/dt = - (A + v_a\sigma_{et}N + r\sigma_a I_e/h\nu_e + \sigma_i I_i/h\nu_i)N_s^* + \sigma_a I_e N/h\nu_e$$
$$dN_s^+/dt = \sigma_i(I_i/h\nu_i)N_s^*; \; N_s^+ + N_s^* + N_s^i = N_{so}$$

Here the term $r\sigma_a \frac{Ie}{h\nu_e}$ = stimulated emission, r is ratio of statistical weights, N_{so} is the initial number density of the selected isotope. Our analysis shows complete ionization across the spatial cross-sectional area of the laser beam can take place if

$$I_e \geqq 10^2 \text{ w/cm}^2$$
$$I_i \geqq 10^5 \text{ w/cm}^2$$
$$\sigma_i > 10^{-16} \text{ cm}^2$$
$$\tau_p \leqq 10^{-7} = \text{laser pulse width}$$

In such a case, the total separated mass in gm/yr of the isotope is given by

$$M = 1 \times 10^{-14}\eta N_{so} L \times S_l/(1 + v_a\sigma_{ct}NT)$$

Here S_l is the mercury flow cross-sectional area covered by laser beams and η is the laser repetion rate per second.

In the case of $\eta = 150$, $L = 10^3$ cm, $S_l = 10$ cm^2, we obtain

$$M = \frac{10^6 P_{Hg}}{(1 + v_a\sigma_{ct}NT)} \quad \text{gm/yr.}$$

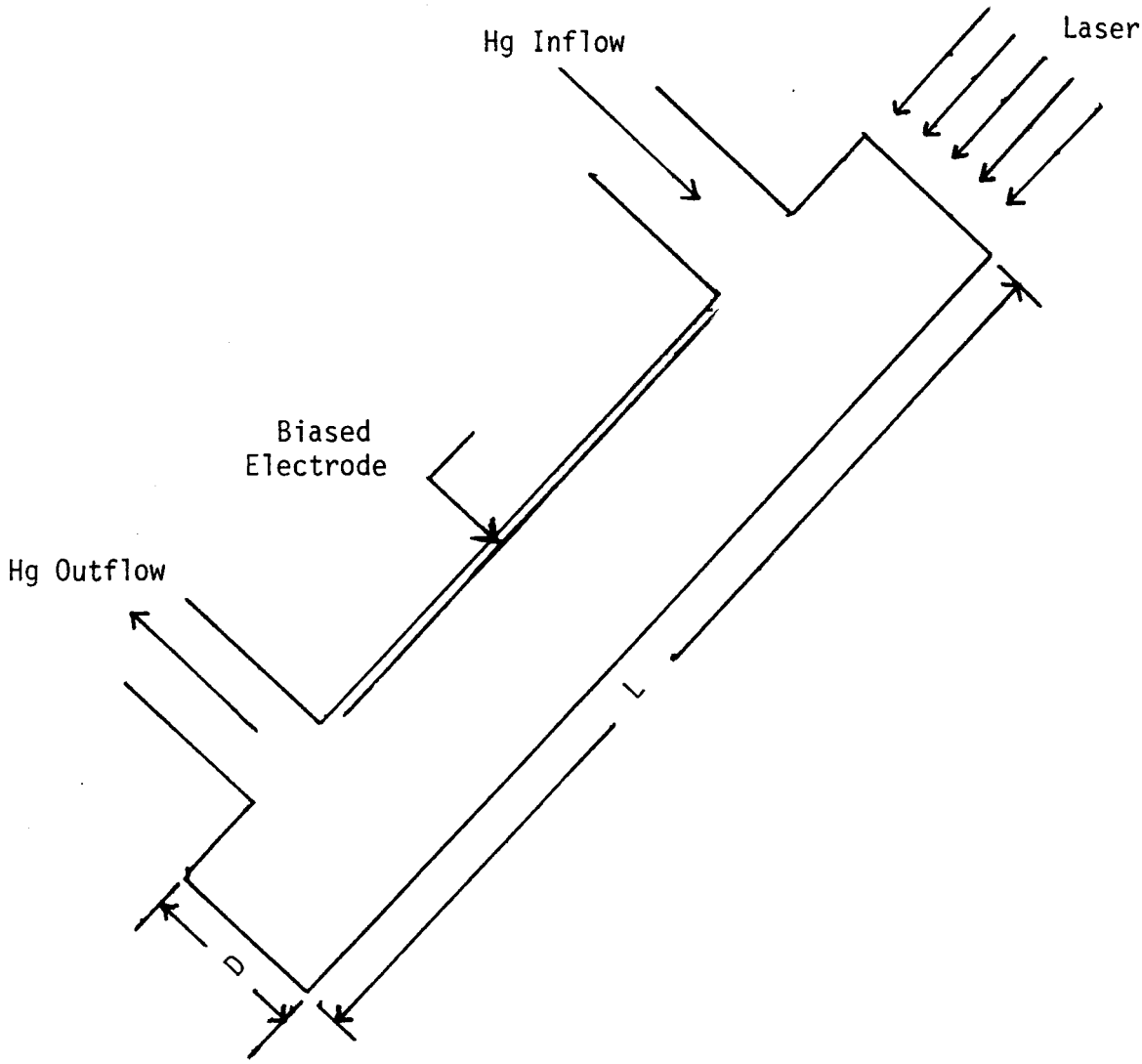

Figure 13. Idealized set-up for preliminary laser photoionization calculations.

The mercury drift velocity can be evaluated as:

$$v_p = 10^4 (E/P_{Hg})^{\frac{1}{2}} \text{ cm/sec}$$

where the electric field intensity E and mercury pressure P_{Hg} are expressed in volt/cm and torr, respectively. For the case of $P_{Hg} = 10^{-1}$ torr, D = 1 cm, E = 10 volt/cm, we obtain

$$M = 10^4 \text{ gm/yr}$$

This value which has been obtained for most favorable conditions is still a factor of 10 less than the desirable amount of Hg isotope. Of course, dark channels, deterioration processes, collection efficiencies, role of dimers, etc., have not been taken into account in these calculations. Furthermore, the very low efficiencies ($\sim < 1\%$) of lasers have not been factored into our calculations. However, from the point of view of obtaining the desired amount of Hg isotopes, utilizing the photoionization method, it appears the yield falls short by one to three orders of magnitude.

It is possible to increase the yield by increasing the electric field and using more powerful lasers. However, increase of the field may reduce isotopic selectivity and increase of laser power may lead to nonlinear porcesses.

2. Utilization of Previous Work

Photochemical isotope selective reactions utilizing mercury and mercury resonance radiation ($^1S_o - ^3P_1$) transition corresponding to 2537Å or 4.89ev or 113 Kcal/mole have been studied extensively by Gunning[4], et al. and recently by Webster and Zare[5] (also referenced therein). Two primary reactions have been found to be most successful in isotope enrichment.

$$HCl + {}^*Hg \rightarrow HgCl + H \text{ (gas phase)}$$

and

$$O_2 + 2{}^*Hg \rightarrow 2HgO\downarrow$$

Most of our work has been based on the HCl reaction with the addition of Butadiene 1,3 C_4H_6. It is believed that C_4H_6, which contains unsaturated carbon hydrogen bonds, removes the H from the gas phase formed in the primary reaction indicated above, and thereby prevents non-isotopic specific reaction from occurring. The possible isotope "scrambling" reactions are as follows

$$H + HCl \rightarrow H_2 + Cl \qquad (1)$$

$$^{N}Hg + Cl \rightarrow HgCl \qquad (2)$$

$$^{N}Hg + H \rightarrow HgH \qquad (3)$$

where ^{N}Hg denotes natural mercury isotopes.

The thermochemical data for reactions (1) and (2) is shown in Table 9.

As shown in Table 10, the primary HCl reaction is not spontaneous and it is excess the 113 kcal/mole provided by the excitation of Hg into the 6^3P_1 state which permits the reaction to occur.

Figure 14 shows the natural mercury 2537Å hyperfine structure for a F40T12 lamp operating at a cold spot temperature of 10°C and due to line broadening, only five peaks appear. Furthermore, the ^{196}Hg peak for natural Hg is not detectable with our present detection system. Utilizing microwave discharge lamps containing high concentrations of individual isotopes, i.e., ^{202}Hg, ^{198}Hg. Gunning obtained enrichments of these particular isotopes of about a factor of 2 with respect to natural mercury. He did not carry out work involving ^{196}Hg enrichment and his work emphasized chemical mechanisms of various photochemical mercury reactions.

Recent work of Webster and Zare[5] demonstrated a factor of 4 enrichment of ^{196}Hg utilizing the HCl reaction. They made use of a natural mercury filter in order to significantly improve the ratio of the ^{196}Hg emission hyperfine line with respect to other hyperfine lines that would normally be emitted from ^{196}Hg microwave emission lamps. The flow reactor cell, to be described, is of similar geometry to what Webster and Zare have reported.

TABLE 9. THERMOCHEMISTRY DATA FOR AN IMPORTANT NON-ISOTOPIC SPECIFIC GAS PHASE REACTION T = 298°K.

Partial Reactions	ΔH_f° Heats of Formation (Kcal/mole)	ΔG_f° Gibbs Free Energy (Kcal/mole)
$HCl \rightarrow \frac{1}{2}Cl_2 + \frac{1}{2}H_2$	+ 22.1	+ 22.778
$H \rightarrow \frac{1}{2}H_2$	- 52.1	- 48.585
$\frac{1}{2}Cl_2 \rightarrow Cl$	+ 29.0	+ 25.102
$H + HCl \rightarrow H_2 + Cl$	- 1.0	- 0.705
$Hg + \frac{1}{2}Cl_2 \rightarrow HgCl$	+ 18.8	+ 13.595
$Cl \rightarrow \frac{1}{2}Cl_2$	- 29.0	- 25.102
$Hg + Cl \rightarrow HgCl$	- 10.2	- 11.507
Net Reaction	Heat of Reaction	
$H + Hg + HCl \rightarrow HgCl + H_2$	- 11.2	- 12.212

TABLE 10. THERMOCHEMISTRY OF PRIMARY HCl REACTION.

Partial Reactions	Change in Heats of Formation (Kcal/mole)	Free Energy Change
$HCl \rightarrow \frac{1}{2}Cl_2 + \frac{1}{2}H_2$	+ 22.1	+22.8
$\frac{1}{2}H_2 \rightarrow H$	+ 52.1	+ 48.6
$Hg + \frac{1}{2}Cl_2 \rightarrow HgCl$	+ 18.8	+ 13.6
Net Reaction	**Heat of Reaction (Kcal/mole)**	**Net Free Energy Change (Kcal/mole)**
$HCl + Hg \rightarrow HgCl + H$	+ 93.0	+ 85.0

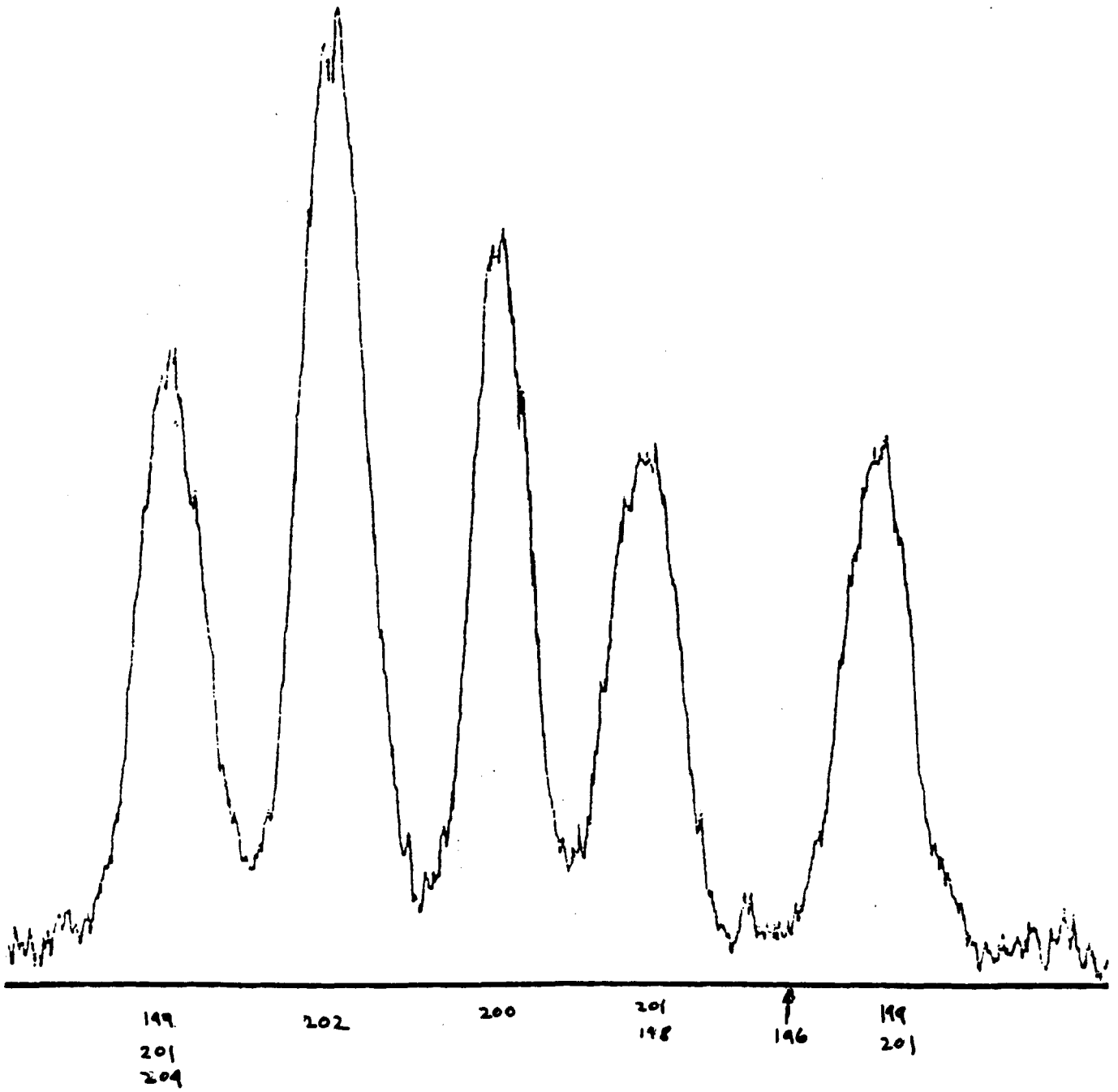

Figure 14. 2537A Spectra for F40T12.

3. Excitation Lamp

Figure 15 is a schematic of the Fabry Perot interferometer system used to observe the 2537 hyperfine structure under different conditions. Not all the lenses are shown in the figure. Typical free spectral range is about 20 GHz with a resolution of about 1 to 2 GHz. The mirror spacing is repetively varied via piezoelectric crystal driven mirror mounts. The monochromator used has ¼ meter focal length, with a U.V blazed holographic grating. This gives an adequately narrow band pass to avoid overlapping orders.

Compared to pressure swept Fabry Perot interferometers, this instrument is very convenient to use and set up, however, it is less stable and has limited certain quantitative measurements. Future use of a calibration lamp and restructuring the optical layout may improve this. Figure 16 shows a spectrum of a microwave lamp containing Hg enriched in the isotope ^{196}Hg. As noted, the other isotopes emit appreciable radiation at the corresponding frequencies. However, use of a ^{N}Hg filter effectively eliminates these other components. The microwave lamp, filter and microwave cavity are shown schematically in Figure 17. Both gas cooling (N_2) and water cooling have been employed with lamps of this type. The natural Hg filter consists of two concentric quartz tubes of about 8 cm length. The microwave lamp passes into the inner cylinder of the filter as shown in Figure 17. In addition to Hg vapor, the cell contains about 7 torr of N_2 which is utilized to prevent re-emission of resonance radiation by the filter. So far attempts to further optimize the filter, for example, by increasing the filter width, has not been shown to increase the lamp filter performance.

4. Static Reactor Experiments

Initial separation experiments were carried out in a static pressure vessel shown schematically in Figure 18 utilizing a ^{198}Hg lamp in order to study principles of enrichment. Table 11 summarizes these results. Here no filtering of the ^{198}Hg lamp was carried out.

5. Flow Reactor Experiments

Figure 19 shows the present flow reactor system. The rotometers control and meter the flow of gas through the system and when a steady state is reached,

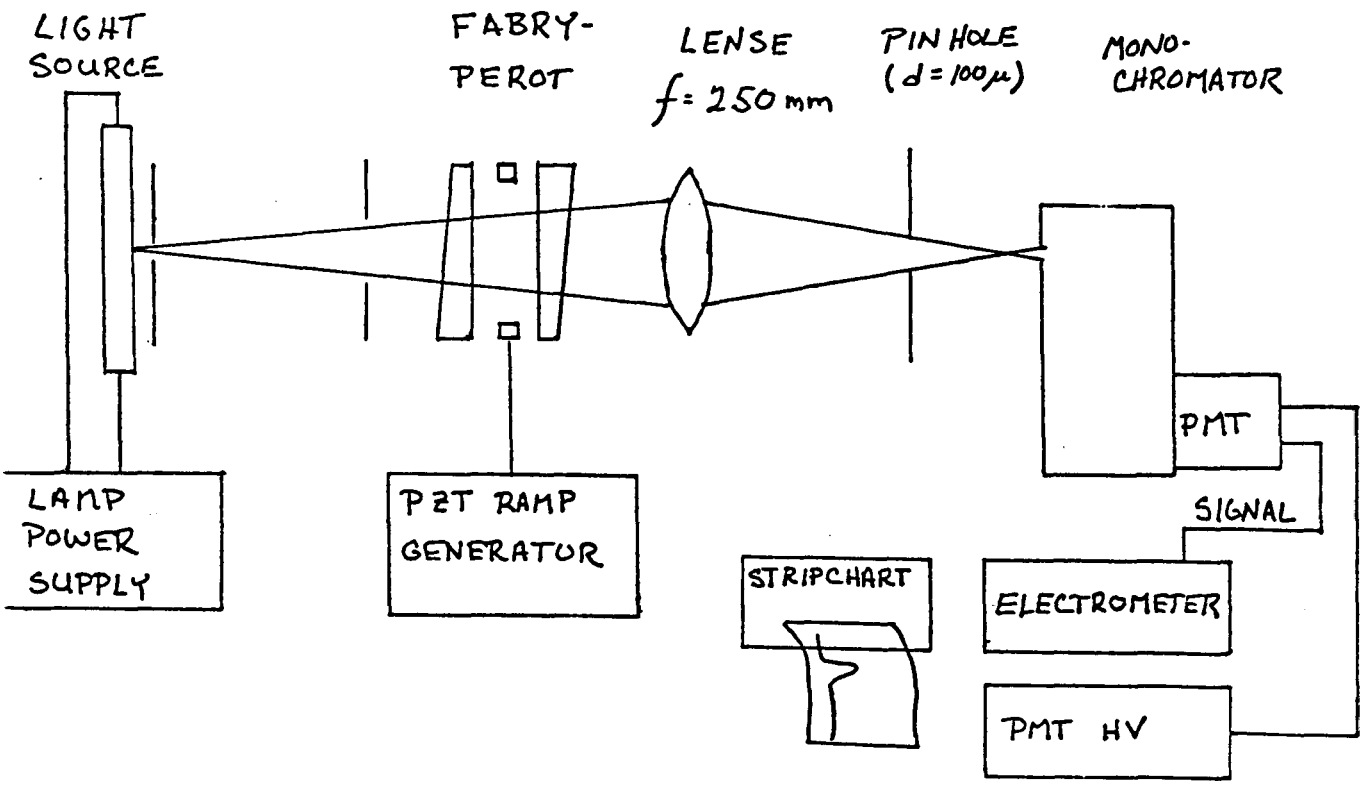

Figure 15. Fabry-Perot interferometer set up.

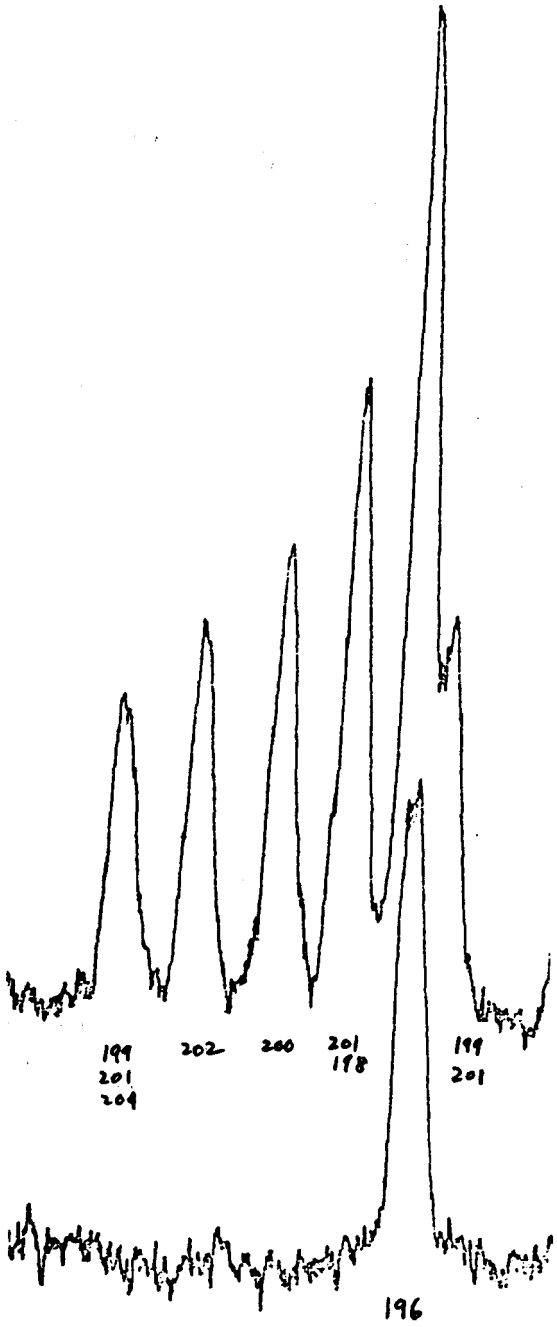

Figure 16. Emission spectrum of the $^3P_1 - ^1S_0$ transition (2537A) of mercury enriched to 35% in the 196 isotope with and without a natural mercury filter.

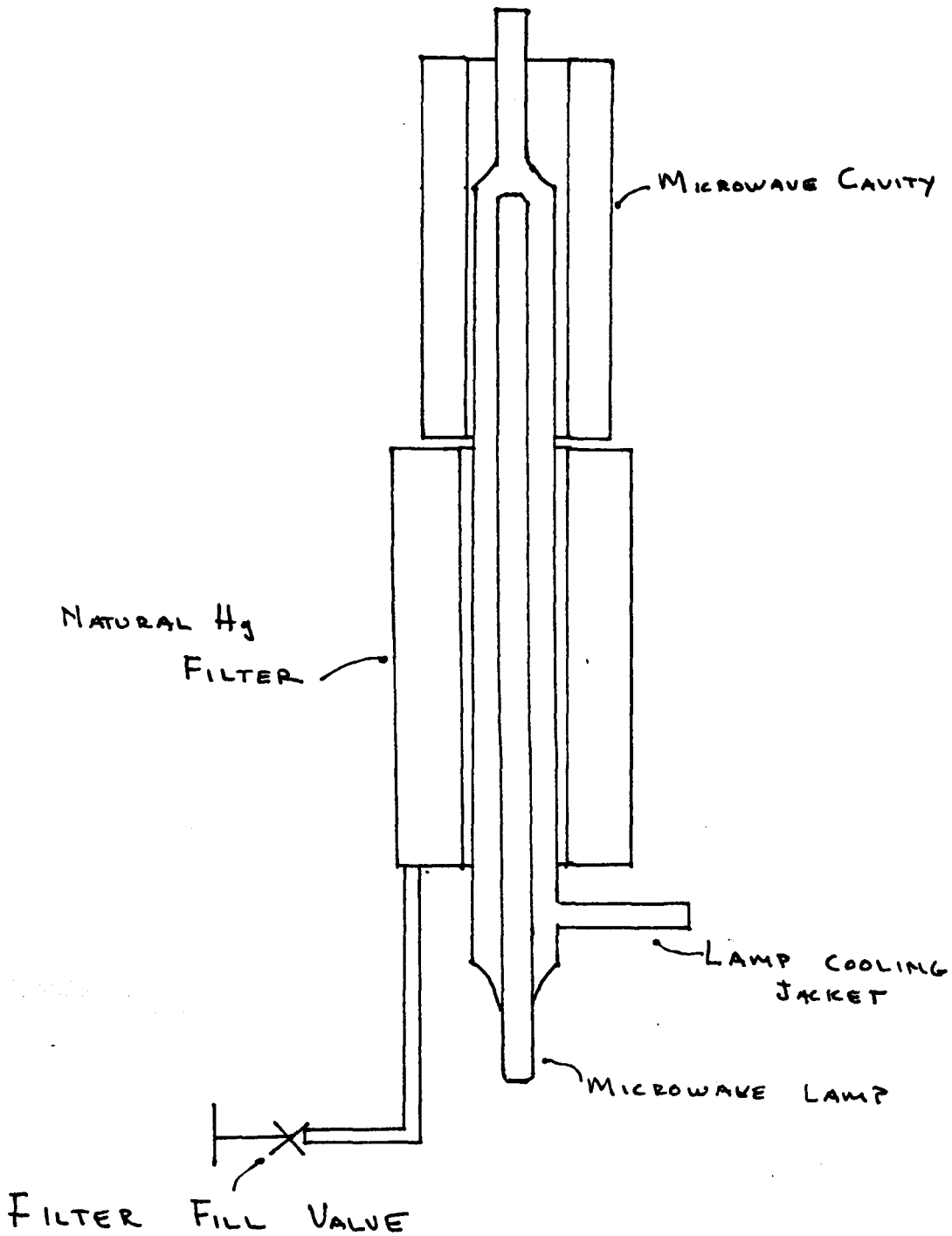

Figure 17. Cutaway Schematic of Microwave Lamp, Cavity and Hg Filter.

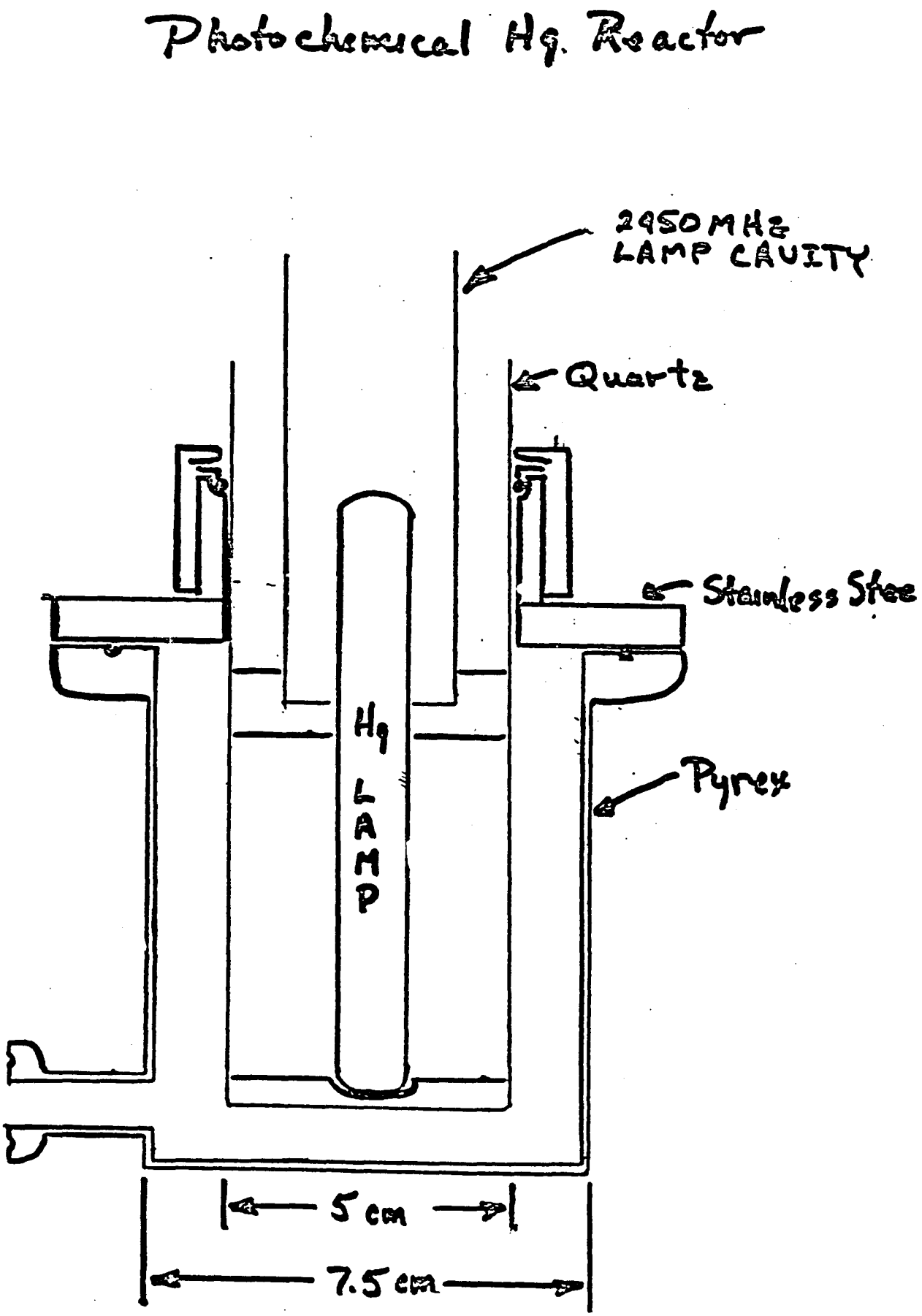

Figure 18. Mercury Photochemical Reactor.

TABLE 11. SUMMARY OF STATIC REACTOR EXPERIMENTS.

Total Pressure (Torr)	5			10			15			20		
Isotope	A	Δ A	% Change	A	Δ A	% Change	A	Δ A	% Change	A	Δ A	% Change
198	10,9	0.9	9.0	11.3	1.3	13.0	13.0	3.0	30.0	19.0	9.0	90.0
199	15.9	-1.2	-7.0	17.2	0.1	0.5	16.2	-0.9	-5.3	14.4	-2.7	-15.2
200	23.0	0.7	3.1	23.7	1.4	6.3	21.6	-0.6	-2.7	19.4	-2.9	-13.0
201	13.4	0.1	0.8	13.8	0.5	3.8	15.2	1.9	14.3	16.8	3.5	25.6
202	30.7	0.2	0.7	28.4	-2.1	-6.9	27.8	-2.6	-8.5	24.6	-5.9	-19.3
204	6.1	-0.7	-10.3	5.6	-1.2	17.6	6.2	-0.6	-8.8	5.8	-1.0	-13.2

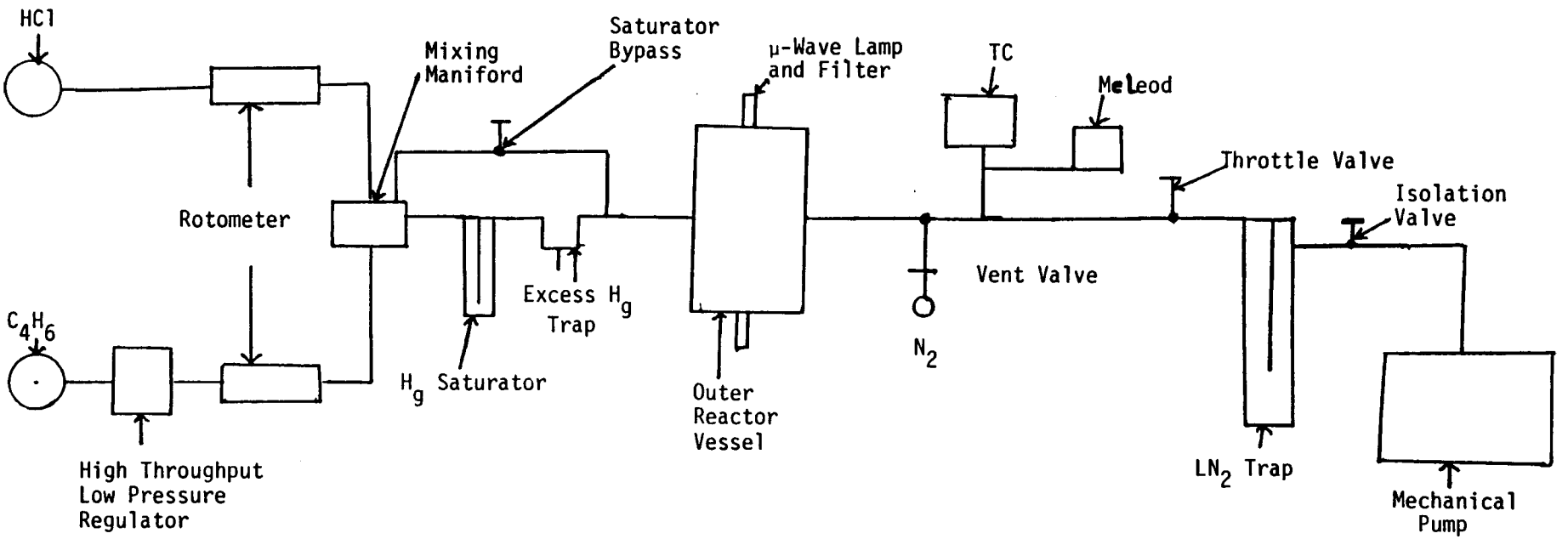

Figure 19. Schematic of Photochemical Flow Reactor.

typically several seconds, this flow is uniform through any section of the gas transfer line. The total pressure in the reactor vessel is controlled by adjustment of the manual throttle valve. A mercury McLeod gauge serves as a reproducible and accurate pressure gauge. Further improvements in the vacuum system and gas handling components can still be carried out. The convecting tubulation, as well as the cold trap and outer reactor vessel, are made of pyrex.

It should be noted that a quartz cylinder (about 5 cm O.D.) concentric with and containing the filter and lamp assembly, shown in Figure 17, passes into two "quick connect" vacuum feedthroughs at the top and bottom of the outer reactor vessel. The outer reactor vessel is also cylindrical and concentric with the quartz cylinder "O" rings mounted in side arms of the outer reactor vessel (about 3 cm I.D.) join the up stream and down stream section of the vacuum system.

The Hg saturator produces additional flow of Hg through the reactor vessel via entrainment of Hg atoms. It should be noted, the use of the saturator is still being investigated and optimized. The saturator by-pass prevents Hg splashing when pumping down and venting the reactor so that the reactor vessel can be removed and the product processed with minimum amount of natural Hg contamination.

6. Collection Methods

The most recent collection method developed utilizes solutions of HCl and either distilled H_2O or CH_3OH (methanol) to plate out the Hg onto a clean copper wire cathode. The plated wire is then placed in a clean tube which is evacuated and the tube tipped off. The wire contained in the completely enclosed and evacuated tube is heated until the Hg deposited on it is vaporized and condensed into one end of the tube. The end of tube containing the liquid Hg is then tipped off to form a small ampule containing the Hg.

7. Sample Analysis

The glass ampule containing the liquid mercury, typically between 0.1 mg to 1.0 mg, is open and the Hg converted to a Ag-Hg amalgam and then is analyzed

via solid probe mass spectrometry. A typical mass spectrum for one scan is shown in Figure 20. For each sample, approximately 10 repetitive scans are taken and peak heights averaged. Frequent calibrations are made via natural Hg samples.

8. Summary and Discussion of Results

Figure 21 summarizes recent flow reactor experiments. Unless otherwise indicated, the C_4H_6:HCl flow ratio is approximately 1:1. The flow rate is 110 SCCM. The calibration of the flow meter was the manufacturers' provided calibration. All measurements shown as a function of lamp temperature are at a total pressure of 1 torr. We note that enrichments of factors 20 to 30 are now being achieved.

Table 12 summarizes trends consistent with the available data and will serve as a guide for future process optimization.

To conclude the photochemical enrichment section, consider the thermochemical data in Tables 9 and 10. As noted in Figure 21, the enrichment increases as the microwave lamp cooling water temperature, and therefore, the inner cylinder temperature increases. Furthermore, the first reaction in the scrambling chain has a particularly small equilibrium constant, whereas, the second is much larger. From Table 10 one would expect the second step in the scrambling chain to be most affected, i.e., decrease in forward direction, by a temperature increase. This may be part of the reason for the enrichment trend in Figure 21.

Changes in the Hg collection or "plating out" of the Hg from the reaction products may also have had an important role in the high enrichment results shown in Figure 21 and is now being investigated.

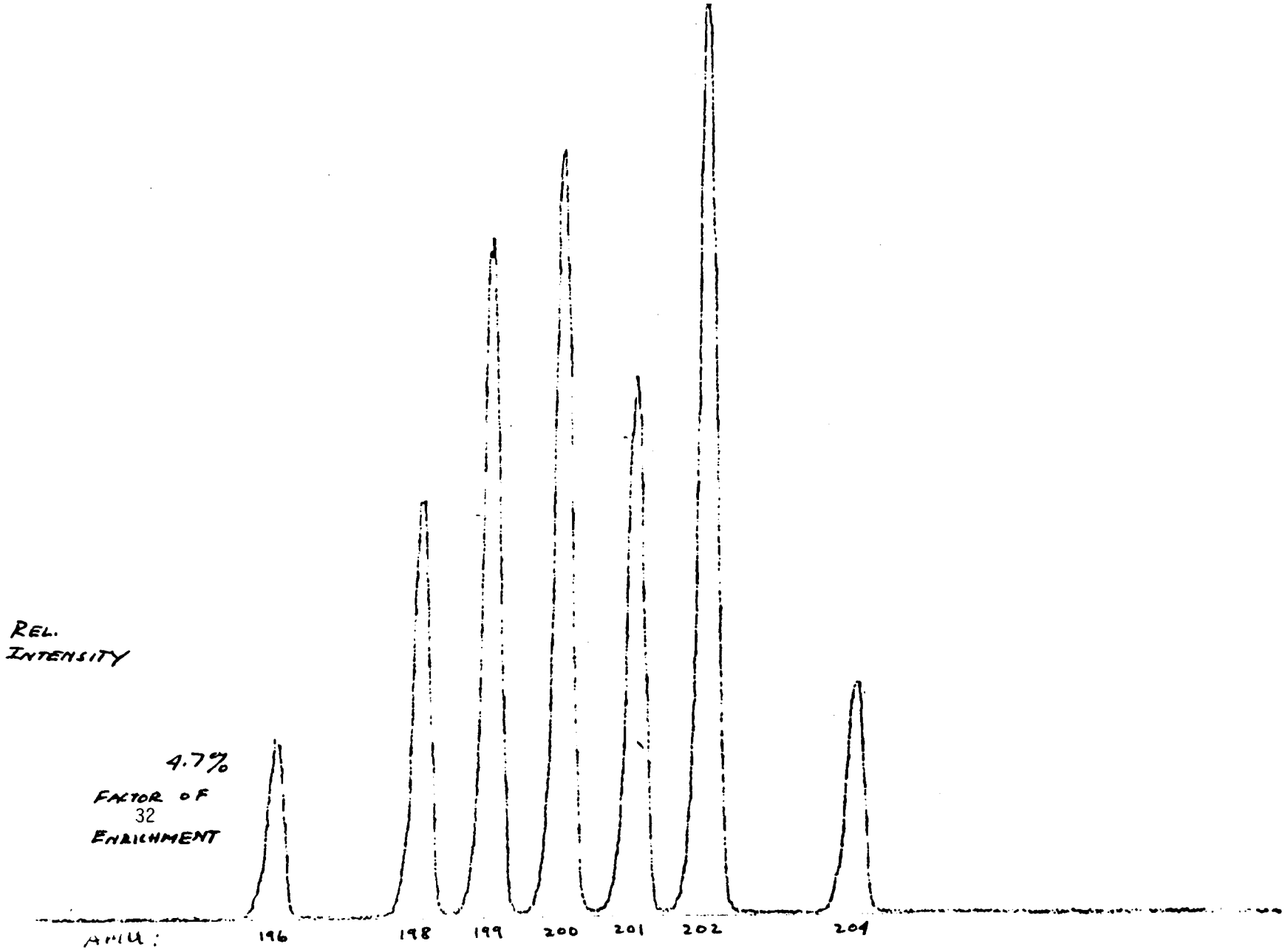

Figure 20. Mass spectrum of single pass enriched mercury.

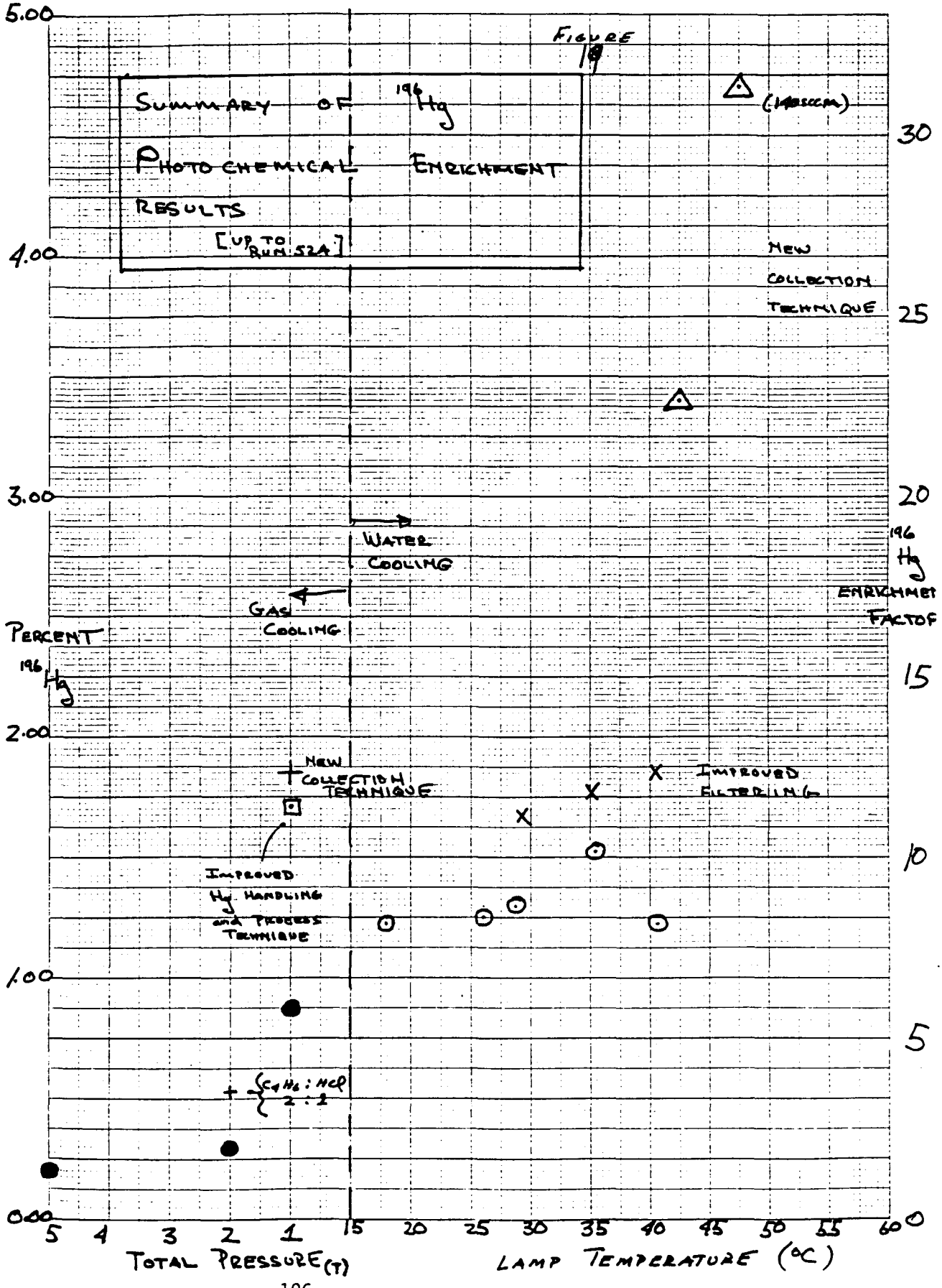

Figure 21. Summary of ^{196}Hg photochemical enrichment results [up to Run 524].

TABLE 12. PARAMETRIC TRENDS FOR PHOTOCHEMICAL STUDIES.

Increasing Independent Variables	Enrichment	Product Yield
HCl:C_4H_6 Flow Ratio	↓	↔
Total Pressure	↓	↑
Total Flow	↔	↑
Lamp Water Cooling Temperature	↑	↔
Enclosure Temperature	↓	↑